concentration of hemoglobin (more than 2 g/L) has also been reported to inhibit ADAMTS13 cleavage [52*]. Plasma concentrations of VWF also potentially affect ADAMTS13 activity; the VWF present in plasma samples would competitively inhibit substrate cleavage. As the plasma concentrations of VWF vary under a subset of pathologic conditions, coexisting pathologies may complicate ADAMTS13 activity assay results.

Factors influencing ADAMTS13 activity
Decreases in ADAMTS13 activity have been reported in liver cirrhosis, chronic uremia, acute inflammatory states, idiopathic thrombocytopenic purpura, disseminated intravascular coagulation, and systemic lupus erythematosus [53,54]. In addition, decreased activity has been observed in the postoperative state, the neonatal period, pregnancy, and aging [47**,53,55,56]. Infusion of the vasopressin analog desmopressin or endotoxin also transiently decreased ADAMTS13 activity [57,58*,59*]. ADAMTS13 activities in control samples exhibit a broad range of values, ranging from 30 to 200% of the mean activity [37,38,47**,51,53,60]. Mild decreases in ADAMTS13 activity in newborns were reported in one study, whereas others have observed normal levels [53,61,62]. Plasma ADAMTS13 activity exhibits a negative correlation with VWF protein and activity levels [53,58*]. Women typically exhibit higher ADAMTS13 activity levels than men [47**].

Sensitivity and specificity of decreased ADAMTS13 activity for diagnosis of thrombotic thrombocytopenic purpura
Severe deficiency in ADAMTS13 activity specifically distinguishes TTP from other thrombotic microangiopathies [63*,64*]. Increasing evidence, however, has questioned the sensitivity of decreased ADAMTS13 activity for diagnosis of TTP and the specificity of ADAMTS13 deficiency as a means to discriminate TTP from other microangiopathies. A population of TTP patients does not exhibit severe ADAMTS13 deficiency [40,53,60,65–67,68*]. These exceptions to the classic correlation between phenotype and genotype in TTP patients have to consider when the ADAMTS13 activity is used for a diagnostic use. These observations may suggest that as-yet-unidentified environmental or genetic factors contribute to the etiology of TTP [5**].

Limitation of assays
Hopefully these new assay methods will be used in clinical practice. Many of these methods, however, still have limitations; with one exception: All these assays use static conditions that do not resemble the physiologic milieu. Each still necessitates a couple of hours to complete and requires special equipment, such as a plate reader. These requirements limit practical use of these assays at a well-equipped institution. All these assays use pooled plasma as a standard, despite the wide range of ADAMTS13

activities among individual plasma samples. Recombinant ADAMTS13 should therefore be used as the standard. For bedside practice in a wide range of clinical settings, simpler and apparatus-free methods are in demand.

Measurements of ADAMTS13 antigen level
ADAMTS13 ELISA kits designed to monitor plasma antigen levels of ADAMTS13 have recently become available from several companies, including Technoclone GmbH and Mitsubishi Kagaku Iatron, Inc. (Tokyo, Japan).

Conclusion
In addition to established assays for ADAMTS13 activity, novel assays using recombinant or synthetic substrates have recently been developed. Although time will be needed to evaluate these analyses, such high-throughput methods will contribute significantly to the accurate diagnosis of microangiopathies, ultimately leading to improved treatment of these diseases. These assays may also help clarify the role of ADAMTS13 in thrombotic disorders, including disseminated intravascular coagulation, stroke, and myocardial infarction. Although severe deficiency in ADAMTS13 activity is an established cause of TTP, recent clinical studies have indicated a more complicated relation of ADAMTS13 deficiency with TTP. Intensive studies of patients with microangiopathies are needed to clarify this discrepancy.

Acknowledgements

References and recommended reading
Papers of particular interest, published within the annual period of review, have been highlighted as:
• of special interest
•• of outstanding interest

1 Moake JL. Thrombotic microangiopathies. N Engl J Med 2002; 347:589–600.

2 George JN, Sadler JE, Lämmle B. Platelets: thrombotic thrombocytopenic purpura. Hematology (Am Soc Hematol Educ Program) 2002:315–334.

3 Lämmle B, George JN. Thrombotic thrombocytopenic purpura: advances in
• pathophysiology, diagnosis, and treatment—introduction. Semin Hematol 2004; 41:1–3.
This article is an introductory remark of special issue of Seminars in Hematology.

4 Sadler JE, Moake JL, Miyata T, et al. Recent advances in thrombotic throm-
•• bocytopenic purpura. Hematology (Am Soc Hematol Educ Program) 2004: 407–423.
This review focused on idiopathic TTP, new ADAMTS13 assays and clinical applications, and the clinical course and long-term outcomes of TTP.

5 Levy GG, Motto DG, Ginsburg D. ADAMTS13 turns 3. Blood 2005. Prepub-
•• lished online.
This review summarizes the progress of TTP and ADAMTS13 analyses since the cloning of the VWF-cleaving protease cDNA in 2001.

6 Furlan M. Proteolytic cleavage of von Willebrand factor by ADAMTS-13 pre-
• vents uninvited clumping of blood platelets. J Thromb Haemost 2004; 2: 1505–1509.
This is a historical sketch on ADAMTS13 by Dr. Furlan, devoted to TTP research.

7 Tsai HM. A journey from sickle cell anemia to ADAMTS13. J Thromb Haemost
• 2004; 2:1510–1514.
This is a historical sketch on ADAMTS13 by Dr. Tsai, devoted to TTP research.

8 Moake JL. Defective processing of unusually large von Willebrand factor mul-
• timers and thrombotic thrombocytopenic purpura. J Thromb Haemost 2004;
2:1515–1521.
This is a historical sketch on ADAMTS13 by Dr. Moake, who discovered ULVWF
multimers in TTP patients' plasma.

9 Soejima K, Nakagaki T. Interplay between ADAMTS13 and von Willebrand
• factor in inherited and acquired thrombotic microangiopathies. Semin Hem-
atol 2005; 42:56–62.
This review deals with the advances in TTP research after the cloning of
ADAMTS13 cDNA in 2001.

10 Gerritsen HE, Robles R, Lämmle B, et al. Partial amino acid sequence of pu-
rified von Willebrand factor-cleaving protease. Blood 2001; 98:1654–1661.

11 Fujikawa K, Suzuki H, McMullen B, et al. Purification of human von Willebrand
factor-cleaving protease and its identification as a new member of the metal-
loproteinase family. Blood 2001; 98:1662–1666.

12 Soejima K, Mimura N, Hirashima M, et al. A novel human metalloprotease syn-
thesized in the liver and secreted into the blood: possibly, the von Willebrand
factor-cleaving protease? J Biochem (Tokyo) 2001; 130:475–480.

13 Zheng X, Chung D, Takayama TK, et al. Structure of von Willebrand factor-
cleaving protease (ADAMTS13), a metalloprotease involved in thrombotic
thrombocytopenic purpura. J Biol Chem 2001; 276:41059–41063.

14 Levy GG, Nichols WC, Lian EC, et al. Mutations in a member of the ADAMTS
gene family cause thrombotic thrombocytopenic purpura. Nature 2001; 413:
488–494.

15 Plaimauer B, Zimmermann K, Volkel D, et al. Cloning, expression, and func-
tional characterization of the von Willebrand factor-cleaving protease
(ADAMTS13). Blood 2002; 100:3626–3632.

16 Kokame K, Miyata T. Genetic defects leading to hereditary thrombotic throm-
• bocytopenic purpura. Semin Hematol 2004; 41:34–40.
This review summarizes the genetic defects and polymorphisms in the
ADAMTS13 gene that have been identified in patients with TTP.

17 Nicholson AC, Malik SB, Logsdon JM Jr, et al. Functional evolution of ADAMTS
• genes: evidence from analyses of phylogeny and gene organization. BMC
Evol Biol 2005; 5:11.
This article describes the phylogenetic relationship between all human ADAMTS
genes, including a comparison with invertebrate and chordate ADAMTS homologues.

18 Suzuki M, Murata M, Matsubara Y, et al. Detection of von Willebrand factor-
• cleaving protease (ADAMTS-13) in human platelets. Biochem Biophys Res
Commun 2004; 313:212–216.
The authors identified ADAMTS13 expression in human platelets.

19 Majerus EM, Zheng X, Tuley EA, et al. Cleavage of the ADAMTS13 propep-
tide is not required for protease activity. J Biol Chem 2003; 278:46643–
46648.

20 Soejima K, Matsumoto M, Kokame K, et al. ADAMTS-13 cysteine-rich/spacer
domains are functionally essential for von Willebrand factor cleavage. Blood
2003; 102:3232–3237.

21 Zheng X, Nishio K, Majerus EM, et al. Cleavage of von Willebrand factor re-
quires the spacer domain of the metalloprotease ADAMTS13. J Biol Chem
2003; 278:30136–30141.

22 Kokame K, Matsumoto M, Soejima K, et al. Mutations and common polymor-
phisms in ADAMTS13 gene responsible for von Willebrand factor-cleaving
protease activity. Proc Natl Acad Sci U S A 2002; 99:11902–11907.

23 Ruan C, Dai L, Su J, et al. The frequency of P475S polymorphism in von
Willebrand factor-cleaving protease in the Chinese population and its rele-
vance to arterial thrombotic disorders. Thromb Haemost 2004; 91:1257–
1258.

24 Bongers TN, De Maat MPM, Dippel DWJ, et al. Absence of Pro475Ser poly-
morphisms in ADAMTS13 in Caucasians. J Thromb Haemost 2005; 3. Pre-
published online.

25 Tao Z, Wang Y, Choi H, et al. Cleavage of ultra-large multimers of von Wil-
• lebrand factor by C-terminal truncated mutants of ADAMTS-13 under flow.
Blood 2005. Prepublished online.
The authors investigated the ADAMTS13 activity of C-terminal-truncated mutants
under flow conditions.

26 Klaus C, Plaimauer B, Studt JD, et al. Epitope mapping of ADAMTS13 auto-
•• antibodies in acquired thrombotic thrombocytopenic purpura. Blood 2004;
103:4514–4519.
The authors examined the epitopes recognized by inhibitory autoantibodies spe-
cific for ADAMTS13 and identified Cys-rich and spacer domains as the major tar-
geted epitopes. CUB domains and first TSP-1 domain also demonstrated some
reactivity.

27 Luken BM, Turenhout EA, Hulstein JJ, et al. The spacer domain of ADAMTS13
contains a major binding site for antibodies in patients with thrombotic throm-
bocytopenic purpura. Thromb Haemost 2005; 93:267–274.

28 Banno F, Kaminaka K, Soejima K, et al. Identification of strain-specific variants
•• of mouse Adamts13 gene encoding von Willebrand factor-cleaving protease.
J Biol Chem 2004; 279:30896–30903.
In mice, two types of ADAMTS13 mutants were present in a strain-specific man-
ner. These mutations are caused by the insertion of an intracisternal A particle ret-
rotransposon introducing a premature stop codon.

29 Crawley JT, Lam JK, Rance JB, et al. Proteolytic inactivation of ADAMTS13 by
•• thrombin and plasmin. Blood 2005; 105:1085–1093.
The authors found that ADAMTS13 is degraded by thrombin and plasmin in vitro,
resulting in the loss of VWF cleaving activity.

30 Sutherland JJ, O'Brien LA, Lillicrap D, et al. Molecular modeling of the
von Willebrand factor A2 domain and the effects of associated type 2A
von Willebrand disease mutations. J Mol Model (Online) 2004; 10:259–
270.

31 Nishio K, Anderson PJ, Zheng XL, et al. Binding of platelet glycoprotein Ibα
•• to von Willebrand factor domain A1 stimulates the cleavage of the adjacent
domain A2 by ADAMTS13. Proc Natl Acad Sci U S A 2004; 101:10578–
10583.
The authors reported a Y1584C mutation, 22 residues N-terminal to the
ADAMTS13 scissile site, within the A2 domain of VWF. Carriers of this
mutation demonstrated increased susceptibility of VWF to proteolysis by
ADAMTS13.

32 Bowen DJ, Collins PW. An amino acid polymorphism in von Willebrand factor
correlates with increased susceptibility to proteolysis by ADAMTS13. Blood
2004; 103:941–947.

33 Bowen DJ, Collins PW, Lester W, et al. The prevalence of the cysteine 1584
variant of von Willebrand factor is increased in type 1 von Willebrand disease:
co-segregation with increased susceptibility to ADAMTS13 proteolysis but
not clinical phenotype. Br J Haematol 2005; 128:830–836.

34 Veyradier A, Girma JP. Assays of ADAMTS-13 activity. Semin Hematol 2004;
• 41:41–47.
This review introduced five ADAMTS13 assay methods.

35 Furlan M, Robles R, Lämmle B. Partial purification and characterization of
a protease from human plasma cleaving von Willebrand factor to fragments
produced by in vivo proteolysis. Blood 1996; 87:4223–4234.

36 Tsai HM. Physiologic cleavage of von Willebrand factor by a plasma protease
is dependent on its conformation and requires calcium ion. Blood 1996;
87:4235–4244.

37 Obert B, Tout H, Veyradier A, et al. Estimation of the von Willebrand factor-
cleaving protease in plasma using monoclonal antibodies to vWF. Thromb
Haemost 1999; 82:1382–1385.

38 Gerritsen HE, Turecek PL, Schwarz HP, et al. Assay of von Willebrand factor
(vWF)-cleaving protease based on decreased collagen binding affinity of de-
graded vWF: a tool for the diagnosis of thrombotic thrombocytopenic purpura
(TTP). Thromb Haemost 1999; 82:1386–1389.

39 Bohm M, Vigh T, Scharrer I. Evaluation and clinical application of a new
method for measuring activity of von Willebrand factor-cleaving metallopro-
tease (ADAMTS13). Ann Hematol 2002; 81:430–435.

40 Remuzzi G, Galbusera M, Noris M, et al. von Willebrand factor cleaving pro-
tease (ADAMTS13) is deficient in recurrent and familial thrombotic thrombo-
cytopenic purpura and hemolytic uremic syndrome. Blood 2002; 100:778–
785.

41 Padilla A, Moake JL, Bernardo A, et al. P-selectin anchors newly released ul-
• tralarge von Willebrand factor multimers to the endothelial cell surface. Blood
2004; 103:2150–2156.
The authors found that ULVWF multimers are anchored to the surface of endothe-
lial cells through P-selectin after stimulation with histamine.

42 Dong JF, Moake JL, Nolasco L, et al. ADAMTS-13 rapidly cleaves newly se-
creted ultralarge von Willebrand factor multimers on the endothelial surface
under flowing conditions. Blood 2002; 100:4033–4039.

43 Dong JF, Whitelock J, Bernardo A, et al. Variations among normal individuals
• in the cleavage of endothelial-derived ultra-large von Willebrand factor under
flow. J Thromb Haemost 2004; 2:1460–1466.
The authors measured ADAMTS13 activity using platelet-decorated ULVWF
strings bound to endothelial cells under flow conditions.

44 Studt JD, Bohm M, Budde U, et al. Measurement of von Willebrand
factor-cleaving protease (ADAMTS-13) activity in plasma: a multicenter
comparison of different assay methods. J Thromb Haemost 2003; 1:1882–
1887.

45 Tripodi A, Chantarangkul V, Bohm M, et al. Measurement of von Willebrand
• factor cleaving protease (ADAMTS-13): results of an international collabora-
tive study involving 11 methods testing the same set of coded plasmas.
J Thromb Haemost 2004; 2:1601–1609.
This international multicenter study evaluated 11 methods measuring ADAMTS13
activity.

46 Kokame K, Matsumoto M, Fujimura Y, *et al.* VWF73, a region from D1596 to
• R1668 of von Willebrand factor, provides a minimal substrate for
ADAMTS-13. Blood 2004; 103:607–612.
Using recombinant techniques, the authors identified the minimal substrate region
for ADAMTS13 cleavage, composed of 73 amino acid residues from the A2 domain of VWF.

47 Kokame K, Nobe Y, Kokubo Y, *et al.* FRETS-VWF73, a fluorogenic substrate
•• for ADAMTS13 assay. Br J Haemost 2005; 129:93–100.
FRETS-VWF73 was developed as a fluorogenic substrate for an ADAMTS13 activity assay using fluorescence resonance energy transfer.

48 Zhou W, Tsai HM. An enzyme immunoassay of ADAMTS13 distinguishes
• patients with thrombotic thrombocytopenic purpura from normal individuals
and carriers of ADAMTS13 mutations. Thromb Haemost 2004; 91:806–811.
Recombinant GST-VWF73-H was used for an ADAMTS13 activity assay.

49 Cruz MA, Whitelock J, Dong JF. Evaluation of ADAMTS-13 activity in plasma
using recombinant von Willebrand Factor A2 domain polypeptide as substrate. Thromb Haemost 2003; 90:1204–1209.

50 Whitelock JL, Nolasco L, Bernardo A, *et al.* ADAMTS-13 activity in plasma is
• rapidly measured by a new ELISA method that uses recombinant VWF-A2
domain as substrate. J Thromb Haemost 2004; 2:485–491.
A recombinant A2 domain of VWF was used for an ADAMTS13 activity assay.

51 Furlan M, Robles R, Galbusera M, *et al.* von Willebrand factor-cleaving protease in thrombotic thrombocytopenic purpura and the hemolytic–uremic
syndrome. N Engl J Med 1998; 339:1578–1584.

52 Studt JD, Hovinga JA, Antoine G, *et al.* Fatal congenital thrombotic thrombo-
• cytopenic purpura with apparent ADAMTS13 inhibitor: in vitro inhibition of
ADAMTS13 activity by hemoglobin. Blood 2005; 105:542–544.
The authors observed that extremely high concentrations of hemoglobin interfere with ADAMTS13 activity.

53 Mannucci PM, Canciani MT, Forza I, *et al.* Changes in health and disease of
the metalloprotease that cleaves von Willebrand factor. Blood 2001; 98:
2730–2735.

54 Moore JC, Hayward CP, Warkentin TE, *et al.* Decreased von Willebrand factor protease activity associated with thrombocytopenic disorders. Blood
2001; 98:1842–1846.

55 Lattuada A, Rossi E, Calzarossa C, *et al.* Mild to moderate reduction of
a von Willebrand factor cleaving protease (ADAMTS-13) in pregnant
women with HELLP microangiopathic syndrome. Haematologica 2003;
88:1029–1034.

56 Sanchez–Luceros A, Farias CE, Amaral MM, *et al.* von Willebrand factor-
cleaving protease (ADAMTS13) activity in normal non-pregnant women,
pregnant and post-delivery women. Thromb Haemost 2004; 92:1320–1326.

57 Reiter RA, Knobl P, Varadi K, *et al.* Changes in von Willebrand factor-cleaving
protease (ADAMTS13) activity after infusion of desmopressin. Blood 2003;
101:946–948.

58 Reiter RA, Varadi K, Turecek PL, *et al.* Changes in ADAMTS13 (von-
• Willebrand-factor-cleaving protease) activity after induced release of von
Willebrand factor during acute systemic inflammation. Thromb Haemost
2005; 93:554–558.
The authors observed that systemic inflammation induced by intravenous infusion of endotoxin decreased after 4 to 24 hours and returned to normal after 7 days.

59 Mannucci PM, Capoferri C, Canciani MT. Plasma levels of von Willebrand
• factor regulate ADAMTS-13, its major cleaving protease. Br J Haematol
2004; 126:213–218.
The authors discovered that individuals with blood group O have higher ADAMTS13 activity than non-O group individuals. In addition, infusion of desmopressin decreased ADAMTS13 activity.

60 Veyradier A, Obert B, Houllier A, *et al.* Specific von Willebrand factor-cleaving
protease in thrombotic microangiopathies: a study of 111 cases. Blood
2001; 98:1765–1772.

61 Tsai HM, Sarode R, Downes KA. Ultralarge von Willebrand factor multimers
and normal ADAMTS13 activity in the umbilical cord blood. Thromb Res
2002; 108:121–125.

62 Schmugge M, Dunn MS, Amankwah KS, *et al.* The activity of the von Wille-
brand factor cleaving protease ADAMTS-13 in newborn infants. J Thromb
Haemost 2004; 2:228–233.

63 Matsumoto M, Yagi H, Ishizashi H, *et al.* The Japanese experience with throm-
• botic thrombocytopenic purpura-hemolytic uremic syndrome. Semin Hematol
2004; 41:68–74.
A total of 290 Japanese patients with TTP-HUS were reported.

64 Hovinga JA, Studt JD, Alberio L, *et al.* von Willebrand factor-cleaving protease
• (ADAMTS-13) activity determination in the diagnosis of thrombotic microan-
giopathies: the Swiss experience. Semin Hematol 2004; 41:75–82.
A total of 396 consecutive patients referred to Dr. Lämmle's laboratory for diagnosis purposes were summarized.

65 Bianchi V, Robles R, Alberio L, *et al.* Von Willebrand factor-cleaving protease
(ADAMTS13) in thrombocytopenic disorders: a severely deficient activity is
specific for thrombotic thrombocytopenic purpura. Blood 2002; 100:710–713.

66 Vesely SK, George JN, Lämmle B, *et al.* ADAMTS13 activity in thrombotic
thrombocytopenic purpura–hemolytic uremic syndrome: relation to present-
ing features and clinical outcomes in a prospective cohort of 142 patients.
Blood 2003; 102:60–68.

67 Snider CE, Moore JC, Warkentin TE, *et al.* Dissociation between the level of
von Willebrand factor-cleaving protease activity and disease in a patient with
congenital thrombotic thrombocytopenic purpura. Am J Hematol 2004;
77:387–390.

68 Peyvandi F, Ferrari S, Lavoretano S, *et al.* von Willebrand factor cleaving pro-
• tease (ADAMTS-13) and ADAMTS-13 neutralizing autoantibodies in 100
patients with thrombotic thrombocytopenic purpura. Br J Haematol 2004;
127:433–439.
The authors investigated 100 patients with TTP, discovering that 48% patients exhibited severely reduced ADAMTS13 activity and 28% showed normal levels.

Zinc and Calcium Ions Cooperatively Modulate ADAMTS13 Activity*

Patricia J. Anderson‡, Koichi Kokame§, and J. Evan Sadler‡1

From the ‡Howard Hughes Medical Institute, Department of Medicine, Washington University School of Medicine, St. Louis, Missouri 63110 and the §National Cardiovascular Center Research Institute, Osaka 565-8565, Japan

ADAMTS13 is a metalloproteinase that cleaves von Willebrand factor (VWF) multimers. The metal ion dependence of ADAMTS13 activity was examined with multimeric VWF and a fluorescent peptide substrate based on Asp^{1596}–Arg^{1668} of the VWF A2 domain, FRETS-VWF73. ADAMTS13 activity in citrate-anticoagulated plasma was enhanced ~2-fold by zinc ions, ~3-fold by calcium ions, and ~6-fold by both ions, suggesting cooperative activation. Cleavage of VWF by recombinant ADAMTS13 was activated up to ~200-fold by zinc ions ($K_{D\,app}$ ~0.5 μM), calcium ions ($K_{D\,app}$ ~4.8 μM), and barium ions ($K_{D\,app}$ ~1.7 mM). Barium ions stimulated ADAMTS13 activity in citrated plasma but not in citrate-free plasma. Therefore, the stimulation by barium ions of ADAMTS13 in citrated plasma appears to reflect the release of chelated calcium and zinc ions from complexes with citrate. At optimal zinc and calcium concentrations, ADAMTS13 cleaved VWF with a $K_{m\,app}$ of 3.7 ± 1.4 μg/ml (~15 nM for VWF subunits), which is comparable with the plasma VWF concentration of 5–10 μg/ml. ADAMTS13 could cleave ~14% of VWF pretreated with guanidine HCl, suggesting that this substrate is heterogeneous in susceptibility to proteolysis. ADAMTS13 cleaved FRETS-VWF73 with a $K_{m\,app}$ of 3.2 ± 1.1 μM, consistent with an ~200-fold decrease in affinity compared with VWF. ADAMTS13 cleaved VWF and FRETS-VWF73 with roughly comparable catalytic efficiency of 55 $\mu M^{-1}\,min^{-1}$ and 18 $\mu M^{-1}\,min^{-1}$, respectively. The striking preference of ADAMTS13 for VWF suggests that substrate recognition depends on structural features or exosites on multimeric VWF that are missing from FRETS-VWF73.

The von Willebrand factor (VWF)[2] cleaving proteinase ADAMTS13 is a member of the ADAMTS (a disintegrin and metalloproteinase with thrombospondin repeats") family (1–3). Since the identification of ADAMTS13, evidence has increased concerning the association of severe ADAMTS13 deficiency with the disease thrombotic thrombocytopenic purpura (TTP) (4–6). TTP is characterized by disseminated microvascular thrombi containing platelets and multimers of VWF, which is a plasma protein that mediates platelet adhesion by tethering platelets to the extracellular matrix (7, 8). In the absence of ADAMTS13 activity, ultra-large multimers of VWF accumulate, causing persistent intravascular platelet aggregation and TTP. Congenital TTP, or

Upshaw-Schulman syndrome, is caused by compound heterozygous or homozygous mutations in the ADAMTS13 gene (2, 9, 10). Acquired idiopathic TTP usually affects adults and is caused predominantly by autoimmune responses to ADAMTS13 (6). The mortality rate is ~90% if untreated; however, plasma exchange therapy has reduced this rate to ~20% (11–13).

Many proteinases of the ADAMTS family are involved in extracellular matrix remodeling, angiogenesis, and development, where they typically cleave large multimeric proteins (14, 15). ADAMTS13 regulates the size of plasma VWF multimers by proteolytic cleavage at Tyr^{1605}–Met^{1606} within the A2 domain of VWF subunits (4, 16). ADAMTS proteinases contain a reprolysin-like zinc metalloproteinase domain, a disintegrin domain, a cysteine-rich and spacer region, several thrombospondin type 1 repeats, and variable C termini, which in ADAMTS13 includes two CUB domains (named for the first identified proteins containing this motif, complement C1r/C1s, Uegf, and Bmp1) (17). The metalloproteinase domain of ADAMTS13 has a putative zinc ion catalytic site ($^{224}HEXXHXXGXXHD^{235}$), one predicted calcium ion-binding site coordinated by residues Glu^{83}, Asp^{173}, Cys^{281}, and Asp^{284}, and a conserved Met^{249} that supports the active site zinc ion in a "Met turn"; these features identify ADAMTS13 as a member of the "metzincin" family (1, 18, 19). The metzincins, which include the homologous matrix metalloproteinases and ADAMs (a disintegrin and metalloproteinase), achieve optimal activity with both zinc and calcium ions (18–22).

The role of divalent metal ions in ADAMTS13 activity is not fully understood. Previous studies of ADAMTS13 activity reported that a combination of barium and calcium ions was optimal for cleavage of VWF (4, 5, 23). The addition of zinc ions has yielded inconsistent results; some studies found no effect, whereas others found that zinc ions restored the activity of EDTA-treated ADAMTS13 (4, 23). In addition, interactions of ADAMTS13 with VWF depend upon ionic strength and pH, but optimal conditions vary considerably among several reports. When assayed at pH 8.0, ADAMTS13 activity was greatest under conditions of low ionic strength (4). Other studies have demonstrated proteolysis of VWF by ADAMTS13 at low ionic strength ($I = 75$ mM) in the absence of added metal ions (6).

The previous studies of ADAMTS13 proteolysis of VWF have established that interactions between the enzyme and substrate are dependent upon metal ions and electrostatic interactions. However, these studies have generally employed reaction conditions unlike those prevailing in vivo. Therefore, the properties of ADAMTS13 were investigated under physiological conditions of pH and ionic strength. The enzyme was found to be activated by calcium and zinc ions at concentrations typical of plasma. Additionally, the $K_{m\,app}$ for VWF was within the range of plasma VWF concentrations, but the $K_{m\,app}$ for a synthetic peptide based on the sequence of cleavage site within the VWF A2-domain was ~210-fold higher. This difference indicates that structural features or

exosites within the native multimeric VWF molecule are required for efficient substrate recognition by ADAMTS13.

EXPERIMENTAL PROCEDURES

Materials—Aliquots of normal human plasma (American Red Cross, St. Louis, MO) were stored at −20 °C until use. One unit of ADAMTS13 activity was defined as the activity in 1 ml of pooled normal human plasma. The concentration of purified human plasma VWF (Laboratoire Français du Fractionnement et des Biotechnologies, Lille, France, generously provided by Claudine Mazurier) in phosphate-buffered saline was determined by absorbance at 280 nm with an absorption coefficient of 1.0 mg ml^{-1} cm^{-1} and correction for light scattering at 340 nm as described (24).

Expression of Recombinant ADAMTS13—A cDNA encoding ADAMTS13 with a C-terminal V5-His tag (1, 25) was cloned into the tetracycline-inducible vector pcDNA4/TO (Invitrogen) at the EcoRI site to yield plasmid p4TO-ADAMTS13. TRex 293 cells (Invitrogen) were transfected with p4TO-ADAMTS13 (1 μg) using Lipofectamine 2000 (Invitrogen). Stable cell lines were maintained in Dulbecco's modified Eagle's medium containing 10% tetracycline-approved fetal bovine serum (Clontech or Invitrogen), 300 μg/ml zeocin, 5 μg/ml blasticidin, 2 mM glutamine, 5 units/ml penicillin, and 5 μg/ml streptomycin. Protein expression was initiated in 70–80% confluent roller bottles with 1 μg/ml tetracycline in Freestyle serum-free media (Invitrogen). The media were centrifuged and filtered, and proteinase inhibitors were added (0.1 μM D-Phe-Pro-Arg-CH$_2$Cl (FPR-CK), 0.1 μM Phe-Phe-Arg-CH$_2$Cl (FFR-CK), 144 μM phenylmethylsulfonyl fluoride. The media were concentrated by ultrafiltration on YM30 membranes (Millipore, Inc.) and dialyzed into an appropriate assay buffer. The concentration of recombinant ADAMTS13 was determined by standardization of Western blots with the V5-tagged Positope protein (Invitrogen) as described (25). The concentration of plasma and recombinant ADAMTS13 also was determined with the ImuBIND ADAMTS13 enzyme-linked immunosorbent assay kit (American Diagnostica, Inc.). The concentrations of plasma ADAMTS13 (0.86–0.96 μg/ml) were comparable with those estimated previously (1 μg/ml) (25). Compared with plasma ADAMTS13 (defined as 100%), the specific activity of recombinant ADAMTS13 was 64% in concentrated conditioned medium and 109% after purification to homogeneity, when assayed with FRETS-VWF73 as described below.[3]

ADAMTS13 Assays—Cleavage of VWF by ADAMTS13 was assessed by Western blotting of the 350-kDa dimer of C-terminal VWF subunit fragments (5, 6). Prior to addition, VWF was preincubated for 30 min at 37 °C in 5 mM Tris-HCl, pH 7.6, 150 mM NaCl, 1.2 M guanidine HCl. The reaction mixtures contained plasma (0.6 nM) or recombinant ADAMTS13 with various metal ion concentrations in 50 mM Hepes, pH 7.4, 50 mM NaCl, in the absence or presence of 10 mM EDTA. Similarly, recombinant ADAMTS13 activity (1 nM) was assessed in mixtures of increasing concentrations of metal ions in 50 mM Hepes, pH 7.4, 150 mM NaCl, and 1 mg/ml bovine serum albumin. Metal ion stock solutions (50 mM) were prepared in distilled water. Some metal ions required the addition of small amounts of HCl for solubility, specifically ZnCl$_2$. All reported metal ion concentrations represent the total concentration added to reactions. In complete reactions containing buffer, substrate, and plasma, Zn^{2+} was <2 μM and Ca^{2+} was <250 μM as determined by inductively coupled plasma spectroscopy (Mayo Clinic, Rochester, MN).

Effects of sodium ions on plasma ADAMTS13 were determined in reaction buffer containing 50 mM Hepes, pH 7.4, 0.25 mM ZnCl$_2$, 5 mM

CaCl$_2$, containing either 150 mM NaCl or 150 mM choline chloride ((2-hydroxyethyl)trimethylammonium chloride), and the effects of ionic strength on plasma ADAMTS13 activity were determined by varying the concentration of NaCl in reaction buffer. The effects of guanidine HCl and urea on the cleavage of VWF were studied by varying the concentration of each chaotropic agent in 50 mM Hepes, pH 7.4, 150 mM NaCl. The reactions were preincubated at 37 °C for 10 min prior to the addition of VWF to a final concentration of 20 μg/ml or 2 μg/ml, followed by incubation at 37 °C for 1 h.

The reactions were quenched by the addition of sample loading buffer (62.5 mM Tris, pH 6.8, 1% SDS, 0.01% bromphenol blue, 5% glycerol (final concentrations)) and analyzed by SDS-PAGE on 4% or 5% gels (Invitrogen or Bio-Rad, respectively). The proteins were transferred to polyvinylidene difluoride membranes by electroblotting, and the 350-kDa product was detected by Western blotting with a 1:2500 dilution of horseradish peroxidase-conjugated rabbit anti-human VWF (DAKO, Carpinteria, CA) (26).

The observed product band densities were quantitated from scanned films using NIH Image 1.61 (rsb.info.nih.gov/nih-image/) or by chemifluorescence detected by a STORM Imager and integration of the peaks using ImageQuantTL (Amersham Biosciences). The reaction rates were calculated from the change in band density (ΔD_{obs}/h). The activity with added metal ions was expressed as a ratio to the activity without added metal ions and analyzed by nonlinear least squares fitting of the quadratic binding equation, with the maximal change in fold activation (ΔFA_{max}) and apparent dissociation constant ($K_{D app}$) as the fitted parameters (27). The stoichiometric factor (n) and concentration of ADAMTS13 were fixed at 1.0 and 1 nM, respectively.

Barium Ion Effects on Citrated and Noncitrated Plasma—Plasma samples were collected from healthy volunteer donors according to a protocol approved by the institutional review board of Washington University School of Medicine. Noncitrated plasma was obtained by collection into 75 μM FPR-CK, 75 μM FFR-CK, 75 μM hirudin (Sigma), and 32 μg/ml corn trypsin inhibitor (Hematologic Technologies, Inc.) (final concentrations) (28). The whole blood was centrifuged at 2000 rpm in a Sorvall 6000 for 15 min, and the recovered plasma was inhibited further by adding an additional 75 μM FPR-CK, 75 μM FFR-CK, and 32 μg/ml corn trypsin inhibitor. VWF was predenatured in 5 mM Hepes, pH 8.0, 1.23 M guanidine HCl, for 30 min at 37 °C. ADAMTS13 (0.6 nM) from citrated or noncitrated plasma was incubated with predenatured VWF (2 μg/ml) in the absence or presence of varying concentrations of BaCl$_2$ in 5 mM Hepes, pH 8.0, at 37 °C for 1 h. Effects of barium ions on 30 nM recombinant ADAMTS13 were assessed in 50 mM Hepes, pH 7.4, 150 mM NaCl, and 1 mg/ml bovine serum albumin. The reactions were quenched by the addition of 50 mM EDTA, pH 8.0, and sample loading buffer and analyzed by gel electrophoresis and Western blotting as described above. The activation of recombinant ADAMTS13 by barium ions was calculated and expressed as a ratio to the activity in the absence of added metal ions, and the data were fitted to the quadratic binding equation as described above for calcium and zinc ions. The stoichiometric factor (n) and concentration of recombinant ADAMTS13 were fixed at 1 and 30 nM, respectively.

Kinetics of VWF Cleavage—The reactions were performed with varying concentrations of VWF with plasma ADAMTS13 (0.6 nM) in assay buffer at 37 °C. The densities of the 350-kDa VWF product band were quantitated as described for metal ion-dependent reactions, and the cleavage rates were calculated as the change in product band density per hour (ΔD_{obs}/h). The rates of product generation as a function of VWF concentration were fit to the Michaelis-Menten equation to determine

---

[3] P. J. Anderson and W. Gao, unpublished observations.

−158−

the apparent Michaelis constant ($K_{m\ app}$) and maximal observed density ($\Delta D_{obs\ max}$).

Progress curve analysis of VWF proteolysis was determined under first order reaction conditions where the [VWF] was ~0.5 × $K_{m\ app}$. The reactions contained 2 μg/ml VWF and 0.6 nM plasma ADAMTS13, in assay buffer at 37 °C. The 350-kDa VWF product band was detected by chemifluorescence. The area of the product band as a percentage of the total area from each lane as a function of time was calculated by integration of peaks using ImageQuantTL software (Amersham Biosciences). The percentage of area was multiplied by the concentration of substrate in the reaction to determine the concentration of the 350-kDa band. The progress curve of the changes in the 350-kDa VWF product band as a function of time was fit to Equation 1 to obtain the apparent first order rate constant (k_{obs}) and the maximum product generated ($[VWF]_{max}$), where $k_{obs} = E \cdot k_{cat}/K_m$(29).

$$[VWF]_t = [VWF]_{max}(1 - e^{-k_{obs}t}) \qquad (1)$$

Kinetics of FRETS-VWF73 Cleavage—A peptide containing the cleavage site of ADAMTS13, consisting of Asp^{1596}–Arg^{1668} of VWF, was synthesized by the Peptide Institute (Osaka, Japan). Two amino acids flanking the cleavage site (Gln^{1599} and Asn^{1610}) were substituted with 2,3-diamino-propionic acid modified with 2-(methylamino)benzoyl and 2,4-dinitrophenol, respectively, as fluorescence resonance energy transfer donor and quencher pairs (30). Fluorescence intensities were measured with a PerkinElmer LS55 using a plate reader accessory in white 96-well plates. Increases in fluorescence intensities ($F_{obs} - F_o = \Delta F$) were recorded with time using an excitation wavelength of 340 nm (5-nm band pass) and an emission wavelength of 450 nm (5-nm band pass). Various concentrations of substrate were incubated with 0.17 nM plasma ADAMTS13 in assay buffer. FRETS-VWF73 (2 μM) was cleaved to completion (17.5 h) to establish the relationship between product concentration and fluorescence intensity (ΔF). The observed velocities (ΔF/min) as a function of substrate concentration were fit to the Michaelis-Menten equation to obtain the maximum velocity (V_{max}) and the $K_{m\ app}$. Nonlinear least squares analyses were performed with Scientist software (Micromath).

Cleavage of 2 μM FRETS-VWF73 by 0.3 nM recombinant ADAMTS13 as a function of calcium and zinc ion concentration was assayed similarly in 50 mM Hepes, pH 7.4, 150 mM NaCl, and 1 mg/ml bovine serum albumin, except the instrument used was a PerkinElmer Victor²V plate reader with 340-nm 25-nm bandwidth excitation filter, and 450-nm 10-nm bandwidth emission filter. The errors in the fitted parameters are reported as ±2 S.D.

RESULTS

Metal Ion Dependence of ADAMTS13 Activity—Previous studies of ADAMTS13 demonstrated that barium and calcium ions enhanced the rate of proteolysis of VWF (4), but these studies employed conditions of pH 8.0 and barium ion concentration (10 mM) that do not occur *in vivo*. Therefore, the metal ion activation of ADAMTS13 from both plasma and recombinant sources was re-evaluated under more physiological conditions. The interactions of metal ions with plasma ADAMTS13 were characterized by analyzing the changes in the density of the 350-kDa VWF cleavage product by Western blotting. In contrast to previous results (4), increasing concentrations of BaCl₂ (up to 5 mM) had little effect on the activity of ADAMTS13 at pH 7.4 (Fig. 1). Similarly, Mg(SO₄) and Cu(SO₄) had little effect on the activity of ADAMTS13 at pH 7.4. Increasing concentrations of CoCl₂, Mn(SO₄), and Ni(SO₄) inhibited ADAMTS13 activity. Calcium ions enhanced the activity by at least ~3-fold (up to 5 mM). Zinc ions enhanced the activity by at least
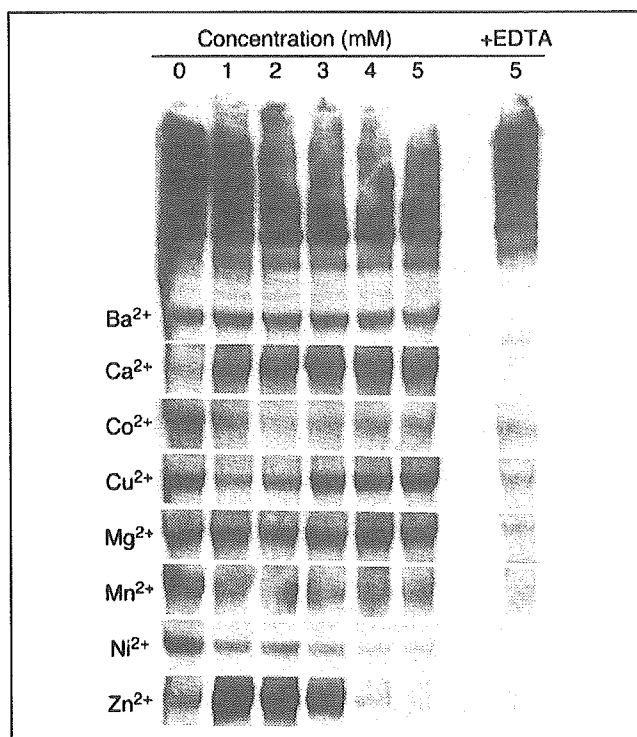

FIGURE 1. **Effects of various divalent metal ions on ADAMTS13 activity at pH 7.4.** ADAMTS13 cleavage of VWF was assessed in the absence or presence of increasing concentrations (up to 5 mM) of BaCl₂, CaCl₂, CoCl₂, CuSO₄, MgSO₄, MnCl₂, NiSO₄, and ZnCl₂. The control assays were performed with 5 mM added metal ion and 10 mM EDTA. The 350-kDa VWF product was detected by gel electrophoresis and Western blotting. The results are representative of at least three experiments.

~2-fold (at 1 mM) (Fig. 1). ADAMTS13 activity was undetectable at concentrations of zinc ions above 3 mM, possibly because of inhibition of the enzyme by $Zn(OH)^+$ (31). Approximately 50% of the susceptible VWF was cleaved in this experiment at the optimal concentrations of CaCl₂ or ZnCl₂, and the extent of activation by these ions is underestimated slightly because of decreases in substrate concentration during the reaction. Nevertheless, the results indicate that low concentrations of zinc or calcium ions enhance the cleavage of VWF by ADAMTS13.

To determine the optimal concentration of zinc ions for plasma ADAMTS13 activity, zinc ion concentrations were varied below 250 μM (Fig. 2A). Increasing concentrations of ZnCl₂ enhanced the activity of ADAMTS13 by ~2-fold. (Fig. 2, A and C). The addition of 5 mM CaCl₂ in the presence of increasing concentrations of ZnCl₂ further enhanced the activity of ADAMTS13 by ~6-fold (Fig. 2, B and C). The ~6-fold increased activation demonstrated ADAMTS13 proteolysis of VWF to be dependent on both zinc and calcium ions and suggested a cooperative role of the two divalent cations.

Partial unfolding of VWF by chaotropic agents such as urea or guanidine HCl is required for rapid cleavage by ADAMTS13 in the absence of fluid shear stress (4–6, 23). To determine the effects of zinc and calcium ions on the proteolysis of VWF under these conditions, VWF was pretreated in varying concentrations of guanidine HCl or urea and then diluted 10-fold into reactions containing ADAMTS13. In the presence of zinc and calcium ions, the optimal concentration of guanidine HCl was between 1.0 and 1.25 M guanidine HCl (initial concentrations) for maximal substrate proteolysis (data not shown), which is similar to previous results (5). In contrast, preincubation of VWF in up to 2 M urea did not accelerate cleavage by ADAMTS13 (data not shown). These results suggest that distinct VWF structures are produced upon incu-
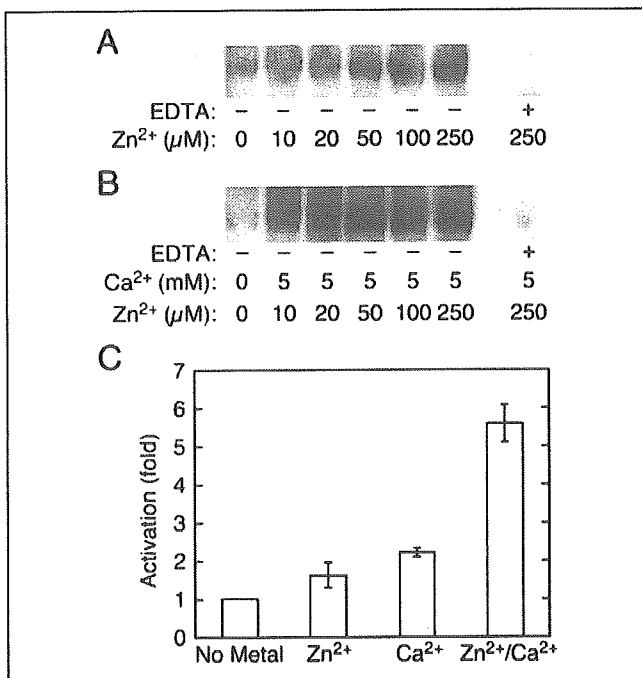
−159−

FIGURE 2. **Activation of ADAMTS13 by zinc and calcium ions.** ADAMTS13 cleavage of plasma VWF was assessed with increasing concentrations of $ZnCl_2$ (μM) in the absence (A) or presence (B) of 5 mM $CaCl_2$ without (−) or with (+) 10 mM EDTA. The 350-kDa VWF product was detected by gel electrophoresis and Western blotting. C, the activation (fold) of ADAMTS13 by 250 μM $ZnCl_2$, 5 mM $CaCl_2$, or both metal ions was determined by densitometric analysis of the Western blots in A and B and in Fig. 1 (for calcium ions alone). The *error bars* represent ± 2 S.D. for the activation (fold) obtained for three concentrations of the varied metal that achieved the greatest activation.

bation with guanidine HCl or urea because the state induced by guanidine HCl persists after dilution, whereas that induced by urea does not.

The assays using citrated plasma as a source of ADAMTS13 activity typically contain ~1 mM citrate (final concentration) (4, 32). Citrate chelates a variety of divalent metal ions and could distort the apparent metal dependence of ADAMTS13 by buffering the concentration of zinc and calcium ions. Therefore, the observed effects of these cations on plasma ADAMTS13 were reassessed with recombinant ADAMTS13, which was free of citrate and other metal ion chelators (Fig. 3). Increasing concentrations of zinc ions enhanced the activity of recombinant ADAMTS13 by ~200-fold, with a $K_{D\,app}$ of 0.5 ± 0.3 μM. Similarly, increasing concentrations of calcium ions enhanced the activity of recombinant ADAMTS13 by ~160-fold, with a $K_{D\,app}$ of 4.8 ± 3.0 μM. The addition of zinc ions to reactions containing near saturating calcium ions (100 μM) further increased ADAMTS13 activity (Fig. 3E). These results indicate a cooperative role for calcium and zinc ions in supporting ADAMTS13 activity.

Effects of Barium Ions on ADAMTS13 Activity—Plasma ADAMTS13 activity is enhanced by the addition of barium ions, when reactions are performed using citrate anticoagulated plasma in low ionic strength buffer at pH 8.0 (4). However, little or no rate enhancement by barium ions was observed at I = 75 mM and pH 7.4 (Fig. 1), and the ability of citrate to buffer divalent metal ions suggested that the reported barium ion effects might not accurately reflect the properties of ADAMTS13. Therefore, the effect of barium ions was determined using plasma samples that were anticoagulated with sodium citrate or with nonchelating inhibitors (FPR-CK, FFR-CK, hirudin, and corn trypsin inhibitor), and reactions were performed in at low ionic strength (I = 2.5–22.5 mM) such that the citrate concentration was either 1 or 0 mM (Fig. 4A). In the presence of citrate, ADAMTS13 activity was enhanced ~2-fold by
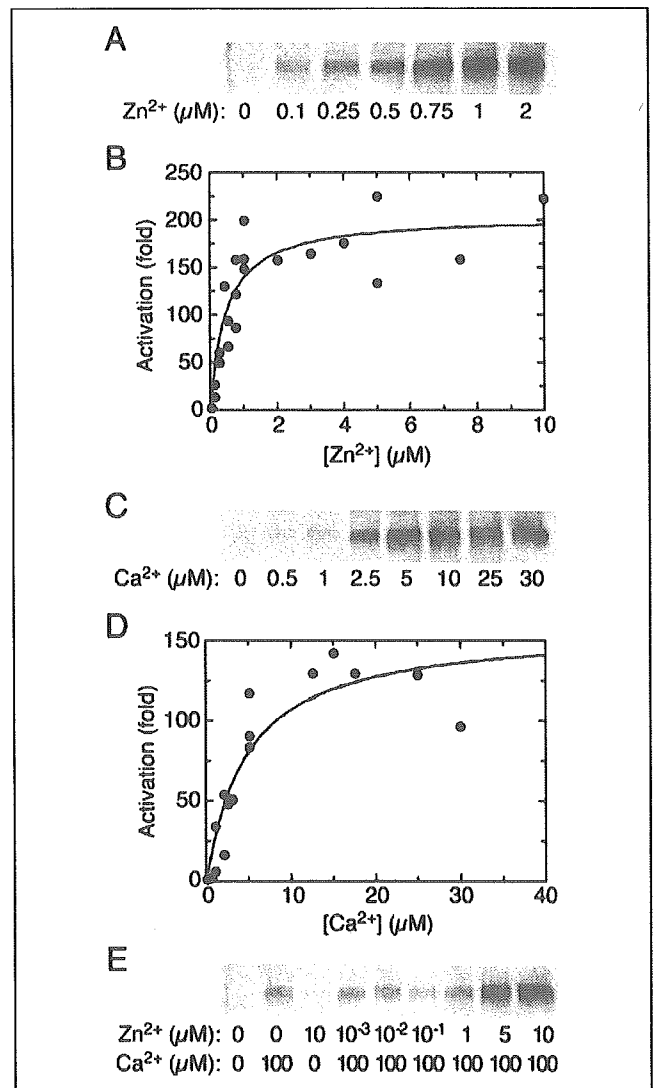

FIGURE 3. **VWF cleavage by recombinant ADAMTS13 and metal ions.** The assays contained recombinant ADAMTS13 (1 nM in A and C and 30 nM in E) and the indicated concentrations of zinc ions (A), or calcium ions (C), or both (E). The 350-kDa VWF cleavage product was detected by gel electrophoresis and Western blotting. The activation (fold) of ADAMTS13 as a function of zinc (B) or calcium (D) ion concentration was determined by chemifluorescence analysis of Western blots from several experiments including those of A and C. The *lines* represent the least squares fit of the quadratic binding equation to the data using the parameters described in the text.

increasing concentrations of barium ions. In the absence of sodium citrate, however, ADAMTS13 activity was not affected by barium ions. Chelation of zinc and calcium ions by citrate also inhibited recombinant ADAMTS13 (Fig. 4B), supporting the conclusion that anticoagulation of plasma by citrate inhibits ADAMTS13.

To avoid the confounding effects of zinc and calcium ions in plasma, activation by barium ions was investigated using recombinant ADAMTS13. Barium ions supported ADAMTS13 activity comparable with that achieved by calcium ions, but with a $K_{D\,app}$ value of 1.7 ± 0.8 mM (Figs. 3D and 4C) that is ~350-fold higher than observed for calcium ions (Fig. 3D).

Effects of Ionic Strength and Sodium Ions on ADAMTS13 Activity—In reactions containing plasma VWF and urea denaturant, ADAMTS13 in citrated plasma is markedly inhibited by increasing ionic strength and is almost inactive in 150 mM NaCl (4). *In vivo*, however, ADAMTS13 must
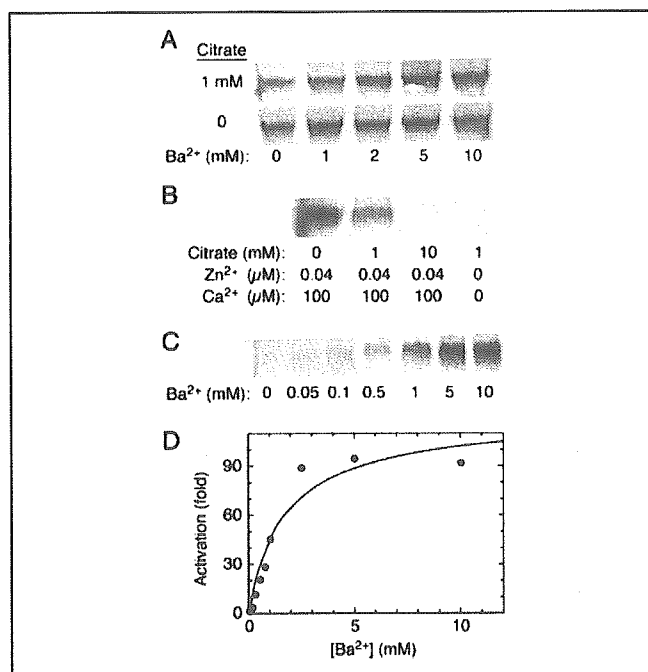
FIGURE 4. **Effects of citrate and barium ions on ADAMTS13 activity at low ionic strength.** *A*, plasma ADAMTS13 (0.6 nM) was assayed in 5 mM Hepes, pH 8.0, with VWF substrate (2 µg/ml) and increasing concentrations of barium ion with or without 1 mM sodium citrate. The 350-kDa VWF cleavage product was detected by gel electrophoresis and Western blotting. *B*, effects of sodium citrate on recombinant ADAMTS13 (30 nM) in the presence and absence of zinc and calcium ions. *C*, recombinant ADAMTS13 (30 nM) was assayed as in *A* with increasing concentrations of barium ions and without sodium citrate. *D*, the activation (fold) of ADAMTS13 as a function of barium ion concentration was determined by chemifluorescence analysis of Western blots from several experiments including those in panel *B*. The maximum extent of VWF cleavage product formed was <15% of total cleavable VWF all conditions. The *line* represents the least squares fit of the quadratic binding equation to the data using the parameters described in the text.
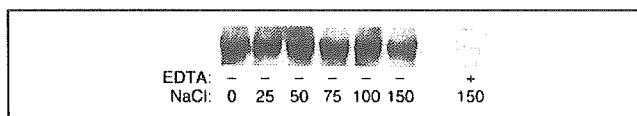

FIGURE 5. **Dependence of ADAMTS13 activity on ionic strength and sodium ion concentration.** Plasma ADAMTS13 was assayed in 50 mM Hepes, pH 7.4, 250 µM ZnCl₂, and 5 mM CaCl₂ with increasing concentrations of sodium chloride (mM) without (−) or with (+) 10 mM EDTA. The 350-kDa VWF cleavage product was detected by gel electrophoresis and Western blotting.
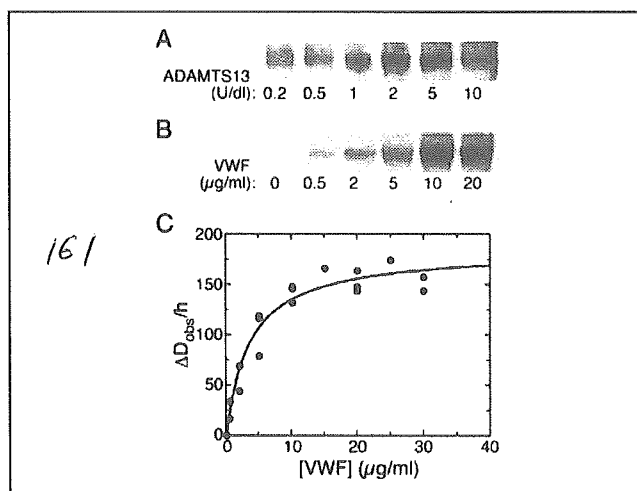

FIGURE 6. **Activity of ADAMTS13 at physiological pH and ionic strength.** *A*, the concentration of plasma ADAMTS13 was varied in reactions (1 h) containing 250 µM ZnCl₂, 5 mM CaCl₂, and a constant VWF concentration (20 µg/ml). *B*, the concentration of VWF was varied in reactions containing 250 µM ZnCl₂, 5 mM CaCl₂, and a constant ADAMTS13 concentration (0.6 nM). *C*, the densities of the 350-kDa product band as a function of VWF concentration were calculated from scanned films for the experiments performed as in *B*. The *line* represents the least squares fit of the Michaelis-Menten equation with the parameters described in the text. Under these conditions, VWF cleavage product generation was linear with time and <15% of susceptible substrate was cleaved during the assay.

operate efficiently at physiological ionic strength. Therefore, the dependence of ADAMTS13 activity on ionic strength was investigated with optimal concentrations of zinc and calcium ions (Fig. 5). Under these conditions ADAMTS13 was fully active at ionic strengths up to $I = 285$ mM (including the contribution of ionized guanidine HCl). Several zinc metalloproteinases and serine proteinases have demonstrated a dependence on sodium ions for activity (33, 34). However, increasing concentrations of sodium chloride, maintaining constant ionic strength with choline chloride, did not alter ADAMTS13 activity (data not shown), indicating that sodium ions do not have a specific effect on ADAMTS13. The results indicate that high ionic strength does not necessarily inhibit ADAMTS13.

Kinetics of VWF Cleavage—The kinetic properties of ADAMTS13 were assessed under conditions approximating physiological pH, ionic strength, and concentrations of zinc and calcium ions. The purified VWF substrate was pretreated with 1.2 M guanidine HCl to induce a conformation susceptible to cleavage (5) and diluted 10-fold into the reaction. Proteolysis of VWF was dependent on both enzyme (Fig. 6*A*) and substrate concentrations (Fig. 6*B*). The rate of proteolysis displayed a hyperbolic dependence on VWF concentration with a $K_{m\,app}$ of 3.7 ± 1.4 µg/ml, or 15 nM in VWF subunits (Fig. 6*C*). ADAMTS13 binds directly to surface-immobilized VWF with a $K_{D\,app}$ of ~4 µg/ml (35), and the concentration of VWF in plasma is ~5–10 µg/ml (36), suggesting that ADAMTS13 functions within a physiological substrate concentration range. The enzyme displayed exponential progress curves at a relatively low VWF concentration of 2 µg/ml (~0.5 × $K_{m\,app}$), consistent with first order reaction kinetics and an apparent first order rate

constant k_{obs} of 0.033 ± 0.021 min⁻¹ and [VWF]ₘₐₓ of 0.34 ± 0.07 µg/ml VWF cleaved (Fig. 7). These results indicate a value for k_{cat} of ~0.83 min⁻¹. This value must be considered a rough estimate because the generation of observed 350-kDa VWF cleavage product requires the cleavage of two adjacent subunits. Determining the true kinetic constants for VWF will require the use of an assay that measures the cleavage of single bonds. Control experiments showed that ADAMTS13 activity was stable for at least 3 h under reaction conditions. Thus, ADAMTS13 cleaves VWF efficiently under physiological conditions of pH, ionic strength, and metal ion concentration. However, a maximum of 14 ± 5% of the total VWF substrate was susceptible to ADAMTS13.

The incomplete cleavage of VWF (Fig. 7) suggested that the substrate was heterogeneous in sensitivity to ADAMTS13 or became resistant during the course of the reaction. To distinguish these possibilities, VWF pretreated with guanidine HCl was diluted 10-fold into reaction buffer and incubated for 100 min prior to the addition of ADAMTS13. Similar reaction kinetics were observed, and a maximum of 6 ± 2% of the substrate was cleaved (data not shown). Thus, the partial cleavage of VWF was reduced ~50% but not eliminated by preincubation without enzyme. The state of the uncleavable VWF is unclear. Denaturation with low concentrations of guanidine may never allow VWF to adopt a cleavable conformation, or upon dilution, some VWF may immediately refold and become resistant to ADAMTS13. These results are consistent with the effects of guanidine HCl on the cleavage of plasma VWF (5) and recombinant VWF (23) by highly purified plasma ADAMTS13.
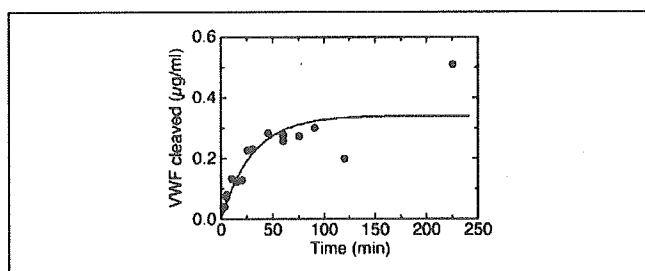
FIGURE 7. **Progress curve for ADAMTS13 cleavage of guanidine-treated VWF.** The concentration of VWF products as a function of time were calculated from the density of the 350-kDa product band by chemifluorescent detection. The reactions contained 2 μg/ml VWF and 0.6 nm plasma ADAMTS13 and were performed as described under "Experimental Procedures." The *line* represents the least squares fit of Equation 1 to the data with the parameters described in the text.

FIGURE 8. **ADAMTS13 cleavage of FRETS-VWF73.** The reactions were performed with 0.15 nm plasma ADAMTS13, and the observed rates of change in fluorescence intensity (ΔF/min) were analyzed as a function of FRETS-VWF73 concentration as described under "Experimental Procedures." Under these conditions, a product concentration of 2 μm corresponds to ~240 ΔF. The *line* represents the least squares fit of the Michaelis-Menten equation with the parameters described in the text.

FRETS-VWF73 Cleavage—The activity of ADAMTS13 toward a structurally homogeneous substrate was investigated using a fluorescent synthetic peptide, FRETS-VWF73, corresponding to residues Asp^{1596}–Arg^{1668} of VWF domain A2 and containing the Tyr^{1605}–Met^{1606} bond cleaved by ADAMTS13 (30). The reactions were performed at approximately physiological pH, ionic strength, and concentrations of zinc and calcium ions. Proteolysis of FRETS-VWF73 was linear with time up to 2 h (data not shown), confirming the stability of ADAMTS13 activity. The reaction demonstrated typical Michaelis-Menten kinetics, with a $K_{m\,app}$ of 3.2 $\pm$ 1.1 μM and V_{max} of 1.04 $\pm$ 0.10 ΔF/min, or a k_{cat} of ~58 min^{-1} (Fig. 8), which is ~70-fold greater than the k_{cat} for VWF cleavage of ~0.83 min^{-1}. The ~210-fold increase in $K_{m\,app}$ compared with multimeric VWF treated with guanidine HCl (Fig. 6) suggests that FRETS-VWF73 lacks tertiary structure or possibly exosites within full-length VWF that may be required for efficient substrate recognition.

The metal ion dependence of FRETS-VWF73 cleavage was qualitatively similar to that of VWF cleavage, although the $K_{D\,app}$ for calcium ion was higher. Activity was undetectable without added metal ions and was increased by calcium ions with a $K_{D\,app}$ of 60 $\pm$ 25 μM. In the presence of 10 μM zinc ions, calcium supported a similar level of activity with a $K_{D\,app}$ of 74 $\pm$ 35 μM (Fig. 9A). Zinc ions alone stimulated ADAMTS13 activity at concentrations <20 μM, but higher concentrations were markedly inhibitory. In the presence of optimal calcium ions, concentrations of zinc ion <10 μM supported full activity, and higher concentrations were inhibitory (Fig. 9B).

Barium ions also stimulated the cleavage of FRETS-VWF73 (2 μM). Normalized to the maximal activity with 10 μM zinc and 1.5 mM calcium ions (100%), the activity observed with 10 mM barium ions was 66%, and that with 10 mM barium plus 10 μM zinc ions was 89%.

DISCUSSION

ADAMTS13 shares several metal ion binding properties with other metalloproteinases. The active site zinc ion of ADAMTS13 binds to the sequence ^{224}HEXXHXXGXXHD^{235} (1), which is common among other metalloproteinases including members of the matrix metalloproteinases and the ADAM families (18, 19, 37). For some metalloproteinases, divalent cations other than zinc can support catalytic activity. For example, reconstitution of apo-stromelysin (MMP-3) with cobalt ions restored the activity by 80% (38), and reconstitution of apo-matrilysin (MMP-7) with manganese, nickel, or cobalt ions also restored activity (39, 40). In addition, calcium, magnesium, and manganese ions have been demonstrated to support procollagen N-proteinase (ADAMTS2) activity, whereas copper and high concentrations of zinc ions inhibit the enzyme (41, 42). Cobalt or copper ions supported the catalytic activity of
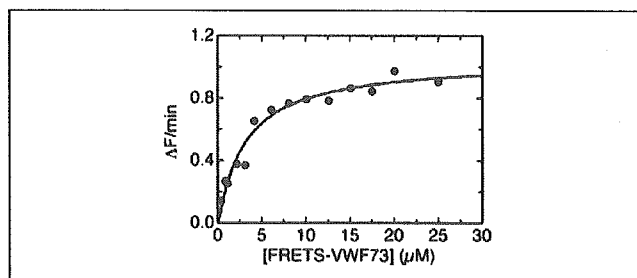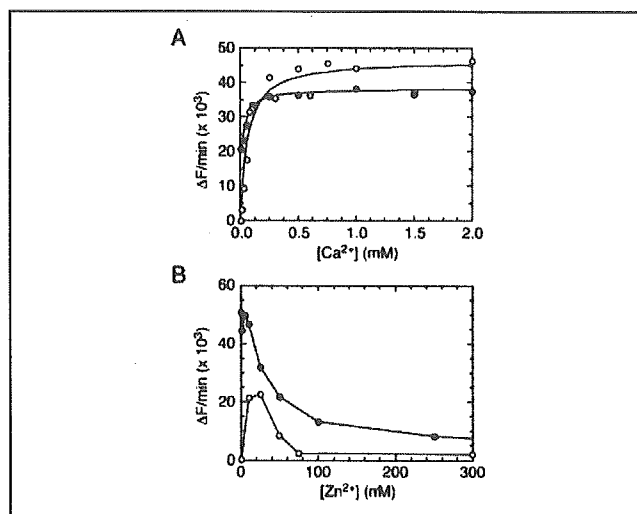

FIGURE 9. **FRETS-VWF73 cleavage by recombinant ADAMTS13 and metal ions.** The assays contained 0.3 nm recombinant ADAMTS13, 2 μm FRETS-VWF73, and various metal ion concentrations. The observed rates of change in fluorescence intensity (ΔF/min) were analyzed as a function of FRETS-VWF73 concentration as described under "Experimental Procedures." The values for ΔF/min were measured on a different fluorometer and cannot be compared with those in Fig. 8. *A*, reactions were performed with the indicated concentration of calcium ions in the absence (*open circles*) or presence (*filled circles*) of 10 μm zinc ions. The *lines* represent the least squares fit of the quadratic binding equation with the parameters described in the text. *B*, reactions were performed with the indicated concentration of calcium ions in the absence (*open circles*) or presence (*filled circles*) of 5 mM calcium ions.

astacin, and the crystal structure showed that these ions had pentagonal bipyriamidal coordination states similar to that of the catalytic zinc ion in native astacin. In contrast, mercury or nickel ions displayed different coordination geometries and inhibited the enzyme (43). In the present study, copper ions slightly enhanced the activity of ADAMTS13, whereas nickel ions inhibited the enzyme and cobalt ions had no effect (Fig. 1). These results are broadly similar to the divalent metal ion effects reported previously for plasma ADAMTS13 under somewhat different assay conditions including pH 8.0, 1 M urea and low ionic strength (4). Additional experiments will be necessary to determine whether divalent metal ions other than zinc can support ADAMTS13 enzyme activity.

Like several other metalloproteinases, ADAMTS13 is inhibited by excessively high concentrations of zinc ions, perhaps because of the formation of Zn(OH)$^+$ that binds to the catalytic Glu or Asp residue within the active site. For example, carboxypeptidase A is inhibited by zinc ions with a K_i of 24 μM (31). The amount of added zinc ions required to activate or inactivate ADAMTS13 depends on the concentration of metal ion chelators. In reactions containing 1 mM EDTA,

–162–

plasma ADAMTS13 was reported to be fully active with 2 mM total zinc ions but inactive with 3 mM zinc ions (23). In the present study, ADAMTS13 in citrated plasma was activated at least ~2-fold by 1 mM zinc ions but was inactive at concentrations >3 mM (Fig. 1), whereas recombinant ADAMTS13 with no added chelators was activated ~200-fold by 5 μM zinc ions (Figs. 3 and 9) and inactivated by >50 μM zinc ions (Fig. 9). This exquisite sensitivity to inhibition by excess zinc ions suggests that ADAMTS13 assays should precisely control the free concentrations of divalent metal ions, particularly in assays developed for clinical use.

Calcium ions play a structural role in many metalloproteinases and stimulate ADAMTS13 activity (4, 5, 23), suggesting a functional interaction between zinc and calcium ion binding. Calcium ions dramatically activate recombinant ADAMTS13 cleavage of VWF and bind with a $K_{D\,app}$ of ~4.8 μM (Fig. 3), well below the plasma free calcium ion concentration of ~1.2 mM. The $K_{D\,app}$ was significantly higher, ~60 μM, when assayed with the FRETS-VWF73 peptide substrate (Fig. 9A). The cause of this difference is not known. Although not studied in detail, the ability of calcium ions alone to stimulate ADAMTS13, a putative zinc-dependent metalloprotease, implies that a very low concentration of zinc ions is present in the dialyzed recombinant enzyme preparations used in these studies (Figs. 3D and 9A) and suggests that zinc and calcium ions bind cooperatively to ADAMTS13. Molecular modeling based on the crystal structures of adamalysin II (44) and ADAM33 (45), which are homologous to ADAMTS13, indicates that calcium ion- and zinc ion-binding sites are located on opposites sides of the ADAMTS13 metalloprotease domain, separated by ~24 Å (1) (data not shown). Therefore, cooperative interactions between the zinc and calcium ions must be mediated indirectly through changes in protein structure. Studies using apo-ADAMTS13 will need to be performed to further establish the role of zinc and calcium ions in the activity of ADAMTS13.

Barium and strontium ions reportedly are more potent than calcium ions for activating ADAMTS13, and clinical ADAMTS13 assays frequently employ supplementation with barium ions (4, 5). The stimulation of ADAMTS13 activity might be due to the occupancy of calcium-binding sites by barium ions, but this explanation probably is incomplete. At low ionic strength (I = 2.5 to 22.5 mM), ADAMTS13 activity in citrated plasma was enhanced ~2-fold by 5–10 mM barium ions (Fig. 4). In contrast, under conditions of physiological ionic strength and pH, the addition of increasing concentrations of barium ions had little or no effect on the activity of ADAMTS13 in citrated plasma (Fig. 1). Barium ions did not enhance ADAMTS13 activity in plasma that was free of citrate (Fig. 4A) and did not stimulate recombinant ADAMTS13 when present at concentrations comparable with the maximally effective concentrations of calcium ions (Fig. 4C). However, much higher levels of barium ions (~5 mM) did stimulate recombinant ADAMTS13 activity (Fig. 4D), suggesting that barium ions can occupy the calcium ion site on ADAMTS13 but with substantially lower affinity. Citrate also inhibits the calcium- and zinc-dependent activity of ADAMTS13 (Fig. 4B). Consequently, the ability of barium ions to activate ADAMTS13 in citrated plasma samples probably is due to the displacement of more potent calcium or zinc ions from complexes with citrate.

These results suggest that sodium citrate is not the optimal anticoagulant for assays of ADAMTS13 activity in blood samples. ADAMTS13 activity is normal in heparinized plasma (5),[4] suggesting that heparin might be an acceptable nonchelating substitute for citrate. Alterna-

tively, anticoagulation may be dispensable because ADAMTS13 appears to be recovered quantitatively in serum (4).

ADAMTS13 is inhibited markedly by increasing ionic strength when assayed in the presence of 1–1.5 M urea (4, 46). However, little or no effect of ionic strength is observed in the absence of urea. Guanidine HCl induces a VWF conformation that is susceptible to ADAMTS13 but also relatively stable after the guanidine HCl concentration is reduced by dilution. The cleavage of guanidine-treated VWF is insensitive to sodium chloride (Fig. 5) or choline chloride (data not shown), indicating that the binding of ADAMTS13 to this form of the substrate does not depend strongly on ionic strength. Although the reaction conditions in these studies vary in other ways that could be significant, a primary role for urea in causing the differences is consistent with the well characterized ability of ionic strength to stabilize proteins against denaturation by urea (47, 48). Consequently, neutral salts like sodium chloride may simply prevent urea-induced changes in the conformation of the VWF substrate that would make it susceptible to ADAMTS13. This conclusion is supported by changes in VWF conformation induced by physiological concentrations of sodium chloride and by other sodium salts, as monitored by intrinsic protein fluorescence (46).

The cleavage of the small fragment of VWF contained in FRETS-VWF73 is relatively insensitive to ionic strength (49) and does not require denaturants (30, 49). This isolated fragment also lacks significant secondary structure by NMR spectroscopy (50). These findings are consistent with the following model in which urea and ionic strength interact and modulate the cleavage of native VWF by ADAMTS13; the transition from a resistant to a susceptible conformation of VWF is facilitated by urea and inhibited by neutral salts, but the recognition and cleavage of the susceptible VWF conformation is largely independent of ionic strength.

Although FRETS-VWF73 does not require denaturation to be cleaved by ADAMTS13, guanidine-treated VWF has a ~210-fold lower $K_{m\,app}$ (Fig. 8). This discrepancy implies that ADAMTS13 interacts with specific, extended structural features of multimeric VWF. Molecular modeling of the A2 domain suggests that it has a characteristic α/β-fold with a six-stranded β-sheet surrounded by three α-helices on each side. The Tyr[1605]–Met[1606] peptide bond is predicted to be buried within the β-sheet, supporting the need for large conformational changes of the A2 domain prior to proteolysis (51, 52). Efficient cleavage also requires the segment Glu[1660]–Arg[1668] in the C-terminal α-helix of the A2 domain (49). The fragment of VWF represented in FRETS-VWF73 corresponds to approximately three β-strands and three α-helices of the A2 domain, but when removed from the context of the complete domain this isolated peptide has no distinct secondary structure (50). Therefore, the relatively poor $K_{m\,app}$ value for FRETS-VWF73 may reflect the large entropic cost of adopting a conformation that can bind ADAMTS13. In addition, such a small fragment of the A2 domain may lack additional sites on VWF that interact with ADAMTS13. For example, the adjacent A1 domain may bind cofactors that affect cleavage (53), and the A3 domain may provide a docking site for ADAMTS13 (54). Such interactions may explain why VWF has both a ~210-fold lower $K_{m\,app}$ and a ~70-fold lower k_{cat} than FRETS-VWF73. These changes have the effect of minimizing the difference in catalytic efficiency ($k_{cat}/K_{m\,app}$) between VWF (55 μM^{-1} min^{-1}) and FRETS-VWF73 (18 μM^{-1} min^{-1}). These kinetic constants must be compared cautiously because the values for VWF are distorted by heterogeneity of the substrate and the complexity of the assay. Nevertheless, independent measurements of ADAMTS13 binding to immobilized VWF (35) yielded an equilibrium constant (K_D = 14 nM, per subunit of VWF) similar to the $K_{m\,app}$ for VWF cleavage of 15 nM.

---

[4] E. A. Tuley and P. J. Anderson, unpublished results.

– 163 –

These studies demonstrate that both plasma and recombinant ADAMTS13 function efficiently under physiological conditions. Once VWF adopts a suitable conformation, perhaps under the influence of fluid shear stress, ADAMTS13 can cleave it rapidly at the pH levels, ionic strengths, and divalent metal ion concentrations that prevail *in vivo*. The ionic strength and denaturant concentrations that are optimal for ADAMTS13 assays *in vitro*, in the absence of fluid shear stress, promote conformational changes in VWF necessary to make it susceptible to cleavage. However, these nonphysiological conditions may impair the recognition of susceptible VWF by ADAMTS13.

The effect of calcium or barium ions on ADAMTS13 activity probably reflects binding to a structural metal ion site in the metalloprotease domain, as predicted by molecular modeling (1) The VWF substrate also might bind calcium ions, but this has not been reported. The VWF A1, A2, and A3 domains do not have MIDAS metal ion sites found in the homologous A domains of certain integrin subunits, and the crystal structures of the VWF A1 and A3 domains do not show metal ions (55, 56). Whether other VWF domains bind metal ions is unknown. Calcium ions are required for optimal cleavage of the FRETS-VWF73 peptide substrate (Fig. 9), which is disordered in solution (50) and presumably unable to bind calcium ions with high affinity. Therefore, calcium ions probably bind directly to ADAMTS13 to stimulate substrate cleavage. Although one calcium site is likely to be in the metalloprotease domain, additional sites in other domains cannot be excluded. For example, the CUB domains in complement component C1s have well defined calcium binding sites (57), suggesting that the two C-terminal CUB domains of ADAMTS13 might have similar sites. Detailed understanding of how ADAMTS13 regulates platelet adhesion should be facilitated by further characterization of the requirements for substrate exposure and recognition by ADAMTS13.

REFERENCES

1. Zheng, X., Chung, D., Takayama, T. K., Majerus, E. M., Sadler, J. E., and Fujikawa, K. (2001) *J. Biol. Chem.* **276**, 41059–41063
2. Levy, G. G., Nichols, W. C., Lian, E. C., Foroud, T., McClintick, J. N., McGee, B. M., Yang, A. Y., Siemieniak, D. R., Stark, K. R., Gruppo, R., Sarode, R., Shurin, S. B., Chandrasekaran, V., Stabler, S. P., Sabio, H., Bouhassira, E. E., Upshaw, J. D., Jr., Ginsburg, D., and Tsai, H. M. (2001) *Nature* **413**, 488–494
3. Soejima, K., Mimura, N., Hirashima, M., Maeda, H., Hamamoto, T., Nakagaki, T., and Nozaki, C. (2001) *J. Biochem. (Tokyo)* **130**, 475–480
4. Furlan, M., Robles, R., and Lammle, B. (1996) *Blood* **87**, 4223–4234
5. Tsai, H. M. (1996) *Blood* **87**, 4235–4244
6. Tsai, H. M., and Lian, E. C. (1998) *N. Engl. J. Med.* **339**, 1585–1594
7. Ruggeri, Z. M. (2003) *J. Thromb. Haemostasis* **1**, 1335–1342
8. Sadler, J. E. (1998) *Annu. Rev. Biochem.* **67**, 395–424
9. Kokame, K., Matsumoto, M., Soejima, K., Yagi, H., Ishizashi, H., Funato, M., Tamai, H., Konno, M., Kamide, K., Kawano, Y., Miyata, T., and Fujimura, Y. (2002) *Proc. Natl. Acad. Sci. U. S. A.* **99**, 11902–11907
10. Moake, J. L. (2004) *Semin. Hematol.* **41**, 4–14
11. Rock, G. A., Shumak, K. H., Buskard, N. A., Blanchette, V. S., Kelton, J. G., Nair, R. C., and Spasoff, R. A. (1991) *N. Engl. J. Med.* **325**, 393–397
12. Rock, G., Porta, C., and Bobbio-Pallavicini, E. (2000) *Haematologica* **85**, 410–419
13. Zheng, X. L., Kaufman, R. M., Goodnough, L. T., and Sadler, J. E. (2004) *Blood* **103**, 4043–4049
14. Tang, B. L. (2001) *Int. J. Biochem. Cell Biol.* **33**, 33–44
15. Nagase, H., and Kashiwagi, M. (2003) *Arthritis Res. Ther.* **5**, 94–103
16. Moake, J. L., Turner, N. A., Stathopoulos, N. A., Nolasco, L. H., and Hellums, J. D. (1986) *J. Clin. Invest.* **78**, 1456–1461
17. Bork, P., and Beckmann, G. (1993) *J. Mol. Biol.* **231**, 539–545
18. Bode, W., Gomis-Ruth, F. X., and Stockler, W. (1993) *FEBS Lett.* **331**, 134–140
19. Stocker, W., Grams, F., Baumann, U., Reinemer, P., Gomis-Ruth, F. X., McKay, D. B., and Bode, W. (1995) *Protein Sci.* **4**, 823–840
20. Vallee, B. L., and Auld, D. S. (1990) *Biochemistry* **29**, 5647–5659
21. Auld, D. S. (2001) *Biometals* **14**, 271–313
22. Chung, D. W., and Fujikawa, K. (2002) *Biochemistry* **41**, 11065–11070
23. Tsai, H.-M., Sussman, I. I., Ginsburg, D., Lankhof, H., Sixma, J. J., and Nagel, R. L. (1997) *Blood* **89**, 1954–1962
24. Girma, J. P., Chopek, M. W., Titani, K., and Davie, E. W. (1986) *Biochemistry* **25**, 3156–3163
25. Zheng, X., Nishio, K., Majerus, E. M., and Sadler, J. E. (2003) *J. Biol. Chem.* **278**, 30136–30141
26. Majerus, E. M., Zheng, X., Tuley, E. A., and Sadler, J. E. (2003) *J. Biol. Chem.* **278**, 46643–46648
27. Bock, P. E., Olson, S. T., and Bjork, I. (1997) *J. Biol. Chem.* **272**, 19837–19845
28. Rand, M., Lock, J., van't Veer, C., Gaffney, D., and Mann, K. (1996) *Blood* **88**, 3432–3445
29. Segel, I. H. (1975) *Enzyme Kinetics: Behavior and Analysis of Rapid Equilibrium and Steady State Enzyme Systems*, Wiley, pp. 39–44, New York
30. Kokame, K., Nobe, Y., Kokubo, Y., Okayama, A., and Miyata, T. (2005) *Br. J. Haematol.* **129**, 93–100
31. Auld, D. S. (1995) *Methods Enzymol.* **248**, 228–242
32. Gerritsen, H. E., Turecek, P. L., Schwarz, H. P., Lammle, B., and Furlan, M. (1999) *Thromb. Haemostasis* **82**, 1386–1389
33. Inouye, K., Lee, S. B., and Tonomura, B. (1996) *Biochem. J.* **315**, 133–138
34. Rose, T., and Di Cera, E. (2002) *J. Biol. Chem.* **277**, 19243–19246
35. Majerus, E. M., Anderson, P. J., and Sadler, J. E. (2005) *J. Biol. Chem.* **280**, 21773–21778
36. Chopek, M. W., Girma, J. P., Fujikawa, K., Davie, E. W., and Titani, K. (1986) *Biochemistry* **25**, 3146–3155
37. Bode, W., and Maskos, K. (2003) *Biol. Chem.* **384**, 863–872
38. Salowe, S. P., Marcy, A. I., Cuca, G. C., Smith, C. K., Kopka, I. E., Hagmann, W. K., and Hermes, J. D. (1992) *Biochemistry* **31**, 4535–4540
39. Cha, J., Pedersen, M. V., and Auld, D. S. (1996) *Biochemistry* **35**, 15831–15838
40. Cha, J., Sorensen, M. V., Ye, Q.-Z., and Auld, D. S. (1998) *J. Biol. Inorg. Chem.* **3**, 353–359
41. Tuderman, L., Kivirikko, K. I., and Prockop, D. J. (1978) *Biochemistry* **17**, 2948–2954
42. Hojima, Y., Behta, B., Romanic, A. M., and Prockop, D. J. (1994) *Matrix Biol* **14**, 113–120
43. Gomis-Ruth, F. X., Grams, F., Yiallouros, I., Nar, H., Kusthardt, U., Zwilling, R., Bode, W., and Stocker, W. (1994) *J. Biol. Chem.* **269**, 17111–17117
44. Gomis-Ruth, F. X., Kress, L. F., Kellermann, J., Mayr, I., Lee, X., Huber, R., and Bode, W. (1994) *J. Mol. Biol.* **239**, 513–544
45. Orth, P., Reichert, P., Wang, W., Prosise, W. W., Yarosh-Tomaine, T., Hammond, G., Ingram, R. N., Xiao, L., Mirza, U. A., Zou, J., Strickland, C., Taremi, S. S., Le, H. V., and Madison, V. (2004) *J. Mol. Biol.* **335**, 129–137
46. De Cristofaro, R., Peyvandi, F., Palla, R., Lavoretano, S., Lombardi, R., Merati, G., Romitelli, F., Di Stasio, E., and Mannucci, P. M. (2005) *J. Biol. Chem.* **280**, 23295–23302
47. Yao, M., and Bolen, D. W. (1995) *Biochemistry* **34**, 3771–3781
48. Maldonado, S., Irun, M. P., Campos, L. A., Rubio, J. A., Luquita, A., Lostao, A., Wang, R., Garcia-Moreno, E. B., and Sancho, J. (2002) *Protein Sci.* **11**, 1260–1273
49. Kokame, K., Matsumoto, M., Fujimura, Y., and Miyata, T. (2004) *Blood* **103**, 607–612
50. Sadler, J. E., Moake, J. L., Miyata, T., and George, J. N. (2004) *Hematology (Am. Soc. Hematol. Educ. Program)*, 407–423
51. Jenkins, P. V., Pasi, K. J., and Perkins, S. J. (1998) *Blood* **91**, 2032–2044
52. Sutherland, J. J., O'Brien, L. A., Lillicrap, D., and Weaver, D. F. (2004) *J. Mol. Model.* **10**, 259–270
53. Nishio, K., Anderson, P. J., Zheng, X. L., and Sadler, J. E. (2004) *Proc. Natl. Acad. Sci. U. S. A.* **101**, 10578–10583
54. Dong, J.-F., Moake, J. L., Bernardo, A., Fujikawa, K., Ball, C., Nolasco, L., Lopez, J. A., and Cruz, M. A. (2003) *J. Biol. Chem.* **278**, 29633–29639
55. Emsley, J., Cruz, M., Handin, R., and Liddington, R. (1998) *J. Biol. Chem.* **273**, 10396–10401
56. Bienkowska, J., Cruz, M., Atiemo, A., Handin, R., and Liddington, R. (1997) *J. Biol. Chem.* **272**, 25162–25167
57. Gregory, L. A., Thielens, N. M., Arlaud, G. J., Fontecilla-Camps, J. C., and Gaboriaud, C. (2003) *J. Biol. Chem.* **278**, 32157–32164

– 164 –

Adiponectin Acts as an Endogenous Antithrombotic Factor

Hisashi Kato, Hirokazu Kashiwagi, Masamichi Shiraga, Seiji Tadokoro, Tsuyoshi Kamae,
Hidetoshi Ujiie, Shigenori Honda, Shigeki Miyata, Yoshinobu Ijiri, Junichiro Yamamoto,
Norikazu Maeda, Tohru Funahashi, Yoshiyuki Kurata, Iichiro Shimomura,
Yoshiaki Tomiyama, Yuzuru Kanakura

Objective—Obesity is a common risk factor in insulin resistance and cardiovascular diseases. Although hypoadiponectinemia is associated with obesity-related metabolic and vascular diseases, the role of adiponectin in thrombosis remains elusive.

Methods and Results—We investigated platelet thrombus formation in adiponectin knockout (APN-KO) male mice (8 to 12 weeks old) fed on a normal diet. There was no significant difference in platelet counts or coagulation parameters between wild-type (WT) and APN-KO mice. However, APN-KO mice showed an accelerated thrombus formation on carotid arterial injury with a He-Ne laser (total thrombus volume: $13.36 \pm 4.25 \times 10^7$ arbitrary units for APN-KO and $6.74 \pm 2.87 \times 10^7$ arbitrary units for WT; $n=10$; $P<0.01$). Adenovirus-mediated supplementation of adiponectin attenuated the enhanced thrombus formation. In vitro thrombus formation on a type I collagen at a shear rate of 250 s^{-1}, as well as platelet aggregation induced by low concentrations of agonists, was enhanced in APN-KO mice, and recombinant adiponectin inhibited the enhanced platelet aggregation. In WT mice, adenovirus-mediated overexpression of adiponectin additionally attenuated thrombus formation.

Conclusion—Adiponectin deficiency leads to enhanced thrombus formation and platelet aggregation. The present study reveals a new role of adiponectin as an endogenous antithrombotic factor. (*Arterioscler Thromb Vasc Biol.* 2006;26:224-230.)

Key Words: acute coronary syndromes ■ obesity ■ platelets ■ thrombosis

O besity is associated with insulin resistance, accelerated atherothrombosis, and cardiovascular diseases.[1,2] Recent studies have revealed that adipose tissue is not only a passive reservoir for energy storage but also produces and secretes a variety of bioactive molecules, known as adipocytokines, including tumor necrosis factor (TNF) α, leptin, resistin, and plasminogen activator inhibitor type-1.[2–4] Dysregulated production of adipocytokines participates in the development of obesity-related metabolic and vascular diseases.[2–4]

Adiponectin is an adipocytokine identified in the human adipose tissue cDNA library, and Acrp30/AdipoQ is the mouse counterpart of adiponectin (reviewed in reference[5]). Adiponectin, of which mRNA is exclusively expressed in adipose tissue, is a protein of 244 amino acids consisting of 2 structurally distinct domains, an N-terminal collagen-like domain and a C-terminal complement C1q-like globular domain. Adiponectin is abundantly present in plasma (5 to 30 μg/mL), and its plasma concentration is inversely related to the body mass index.[5] Plasma adiponectin levels decrease in obesity, type 2 diabetes, and patients with coronary artery disease (CAD).[5–9] Indeed, adiponectin (APN) knockout (KO) mice showed severe diet–induced insulin resistance.[10] In cultured cells, we have demonstrated that human recombinant adiponectin inhibited the expression of adhesion molecules on endothelial cells, the transformation of macrophages to foam cells, and TNF-α production from macrophages.[5,11] Furthermore, APN-KO mice showed severe neointimal thickening in mechanically injured arteries.[12] Adenovirus-mediated supplementation of adiponectin attenuated the development of atherosclerosis in apolipoprotein E–deficient mice as well as postinjury neointimal thickening in APN-KO mice.[12,13] These data suggest the antiatherogenic properties of adiponectin, and, hence, hypoadiponectinemia may be associated with a higher incidence of vascular diseases in obese subjects. Although it is also possible that an altered hemostatic balance may contribute to the pathogenesis of acute cardiovascular events in such patients, the roles of adiponectin in hemostasis and thrombosis remains elusive.

Here we have provided the first evidence that adiponectin affects thrombus formation, and, hence, hypoadiponectinemia may directly contribute to acute coronary syndrome. Our data indicate a new role of adiponectin as an antithrombotic factor.

Methods

Mice
APN-KO male mice (8 to 12 weeks old) were generated as described previously.[10,12] We analyzed mice backcrossed to C57BL/6 for 5 generations.[10,12]

Preparation of Mouse Platelets and Measurement of Coagulation Parameters
Mouse platelet-rich plasma (PRP) was obtained as described previously.[14] Coagulation parameters were measured by SRL Inc.

Platelet Aggregation Study, Adhesion Study, and Flow Cytometry
Platelet aggregation and platelet adhesion study was performed as described previously.[14] Integrin $\alpha_{IIb}\beta_3$ activation and α-granule secretion of wild-type (WT) and APN-KO platelets were detected by phycoerythrin-conjugated JON/A monoclonal antibody (mAb), which binds specifically to mouse-activated $\alpha_{IIb}\beta_3$ (Emfret Analytics) and FITC-conjugated anti-P-selectin mAb (Becton Dickinson), respectively.[14]

Assessment of Atherosclerosis and Bleeding Time Measurement
Assessment of atherosclerosis was performed as described previously.[15] The tail of anesthetized mice (nembutal 65 mg/kg; 8 to 12 weeks old) was transected 5 mm from the tip and then immersed in 0.9% isotonic saline at 37°C. The point until complete cessation of bleeding was defined as the bleeding time.

He-Ne Laser–Induced Thrombosis
The observation of real-time thrombus formation in the mouse carotid artery was performed as described previously.[15] Anesthetized mice (nembutal 65 mg/kg) were placed onto a microscope stage, and the left carotid artery (450 to 500 μm in diameter) was gently exposed. Evans blue dye (20 mg/kg) was injected into the left femoral artery via an indwelt tube, and then the center of the exposed carotid artery was irradiated with a laser beam (200 μm in diameter at the focal plane) from a He-Ne laser (Model NEO-50MS; Nihon Kagaku Engineering Co, Ltd). Thrombus formation was recorded on a videotape through a microscope with an attached CCD camera for 10 minutes. The images were transferred to a computer every 4 s, and the thrombus size was analyzed using Image-J software (National Institutes of Health). We calculated thrombus size by multiplying each area value and its grayscale value together. We then regarded the total size values for an individual thrombus obtained every 4 s during a 10-minute observation period as the total thrombus volume and expressed them in arbitrary units.

Flow Chamber and Perfusion Studies
The real-time observation of mural thrombogenesis on a type I collagen-coated surface under a shear rate of 250 s^{-1} was performed as described previously.[16] Briefly, whole blood obtained from anesthetized mice was anticoagulated with argatroban, and then platelets in the whole blood were labeled by mepacrine. Type I collagen-coated glass cover slips were placed in a parallel plate flow chamber (rectangular type; flow path of 1.9-mm width, 31-mm length, and 0.1-mm height). The chamber was assembled and mounted on an epifluorescence microscope (Axiovert S100 inverted microscope, Carl Zeiss Inc) with the computer-controlled z-motor (Ludl Electronic Products Lts). Whole blood was aspirated through the chamber, and the entire platelet thrombus formation process was observed in real time and recorded with a video recorder.

Preparation of Adenovirus and Recombinant Adiponectin
Adenovirus producing the full-length mouse adiponectin was prepared as described previously.[10] Plaque-forming units (1×10^8) of adenovirus-adiponectin (Ad-APN) or adenovirus-β-galactosidase (Ad-βgal) were injected into the tail vein. Experiments were performed on the fifth day after viral injection. The plasma concentrations of adiponectin were measured by a sandwich ELISA. Mouse and human recombinant proteins of adiponectin were prepared as described previously.[11,17]

RT-PCR
Total cellular RNA of platelets from WT or APN-KO mice was obtained, and contaminated genomic DNA was removed using a QuantiTect Reverse-Transcription kit (QIAGEN). One microgram of total RNA was used as a template for RT-PCR as described previously.[18] For the amplification of transcripts of mouse adiponectin receptors AdipoR1 and AdipoR2, the following primers were used: mouse AdipoR1 5'-ACGTTGGAGAGTCATCCCGTAT-3' (sense) and 5'-CTCTGTGTGGATGCGGAAGAT-3' (antisense) and mouse AdipoR2 5'-TGCGCACACATTTCAGTCTCCT-3' (sense) and 5'-TTCTATGATCCCCAAAAGTGTGC-3' (antisense).[19,20] For human platelet isolation, PRP obtained from 50 mL of whole blood was passed through a leukocyte removal filter as described previously.[21] This procedure removed >99.9% of the contaminated leukocytes.[21] For human AdipoR1 and AdipoR2, the following primers were used: human AdipoR1 5'-CTT-CTACTGCTCCCCACAGC-3' (sense) and 5'-GACAAAGCCCT-CAGCGATAG-3' (antisense) human AdipoR2 5'-GGACCGAGCA-AAAGACTCAG-3' (sense) and 5'-CACCCAGAGGCTGCTACTTC-3' (antisense). In addition, total cellular RNA obtained from a megakaryocytic cell line, CMK, and that from a human monocytic cell line, THP-1 (positive control)[22] was examined in parallel. RT-PCR samples omitting reverse transcriptase were used as negative controls.

Statistical Analysis
Results were expressed as mean±SD. Differences between groups were examined for statistical significance using Student t test.

Results

Characteristics of Adiponectin-Deficient Mice and Assessment of Atherosclerotic Lesions
The basal profiles of APN-KO male mice have been previously described.[10,12] To exclude the effects of diet on APN-KO mice, we used APN-KO male mice (8 to 12 weeks old) fed on a normal diet in this study. There were no differences in platelet counts, PT, APTT, and plasma fibrinogen concentrations (Table I, available online at http://atvb.ahajournals.org). Histological analyses revealed that neither Oil Red O staining of the inner surface of whole aorta nor elastin-van Gieson staining of transverse sections of carotid arteries showed any apparent atherosclerotic lesions in WT or APN-KO mice (data not shown).

Bleeding Time in APN-KO Mice
To examine the effects of adiponectin deficiency on thrombosis and hemostasis, we studied bleeding time in APN-KO mice. The bleeding time in APN-KO mice was slightly but significantly shorter (96.9±34.9 s; n=30; $P<0.05$) than that in WT mice (130.9±52.1 s; n=30).

Enhanced Thrombus Formation in APN-KO Mice and Adiponectin Adenovirus Ameliorates the Thrombogenic Tendency
We next examined the effect of adiponectin deficiency on thrombus formation using the He-Ne laser-induced carotid
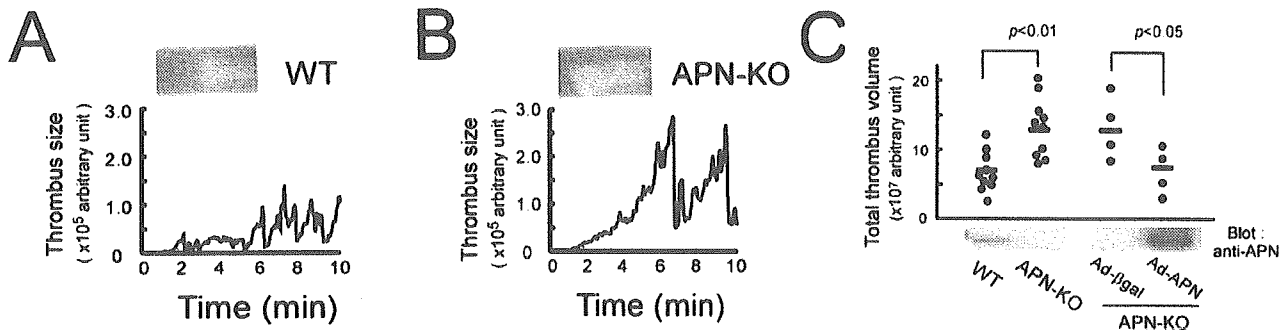
Figure 1. He-Ne laser–induced thrombus formation and adenovirus-mediated supplementation of adiponectin. Anesthetized mice were injected with Evans blue dye followed by irradiation with the He-Ne laser at the exposed left carotid artery. The representative time course of thrombus formation in (A) WT or (B) APN-KO mice is shown. (C) The total thrombus volume was significantly larger in APN-KO mice (n=10; $P<0.01$). In another set of experiments, administration of adenovirus-producing mouse adiponectin (Ad-APN) significantly attenuated the total thrombus volume, as compared with control adenovirus (Ad-βgal)-infected APN-KO mice (n=4; $P<0.05$). Plasma adiponectin levels detected in immunoblots are shown in the lower panel.

artery thrombus model. Endothelial injury of the carotid artery was induced by the interaction of Evans blue dye with irradiation from the He-Ne laser. In WT mice, thrombus formation started 61.0 ± 25.0 s after the initiation of He-Ne laser irradiation (n=10). When the thrombi reached a certain size, they frequently ruptured and detached themselves from the wall because of increased shear stress. Thus, thrombus formation in this in vivo model showed a cyclic fluctuation, and complete occlusion was not observed (Figure 1). During a 10-minute observation period, the cycles of thrombus formation were 8.5 ± 2.3 in WT mice. In APN-KO mice, there was no significant difference in the initiation time for thrombus formation (54.8 ± 8.9 s; n=10; $P=0.46$). However, the cycles of thrombus formation during the 10-minute observation period were significantly fewer (5.4 ± 2.0; n=10; $P<0.01$) in APN-KO mice. The thrombi in APN-KO mice grew larger and appeared to be stable and more resistant to the increased shear stress. Accordingly, the total thrombus volume was significantly larger in APN-KO mice ($6.74\pm2.87\times10^7$ arbitrary units in WT mice and $13.36\pm4.25\times10^7$ arbitrary units in APN-KO mice; n=10; $P<0.01$).

To confirm that adiponectin deficiency is responsible for the enhanced thrombus formation in APN-KO mice, we injected Ad-βgal or Ad-APN into APN-KO mice. On the fifth day after adenoviral injection, we confirmed the elevated plasma adiponectin level in Ad-APN-infected APN-KO mice in an ELISA assay (48.7 ± 6.8 μg/mL; n=4), as well as in an immunoblot assay. In the carotid artery thrombus model, the total thrombus volume in Ad-βgal-infected APN-KO was $12.94\pm4.67\times10^7$ arbitrary units, which was compatible with that of APN-KO mice shown in Figure 1. In contrast, Ad-APN infection significantly decreased the total thrombus volume in APN-KO mice ($6.23\pm3.09\times10^7$ arbitrary units; n=4; $P<0.05$). These results indicate that adiponectin deficiency is responsible for the thrombogenic tendency in vivo.

Platelet-Thrombus Formation on Immobilized Collagen Under Flow Conditions

Because endothelial function may affect in vivo thrombus formation, we next performed in vitro mural thrombus formation on a type I collagen-coated surface under flow conditions. Figure 2 shows thrombus formation during a
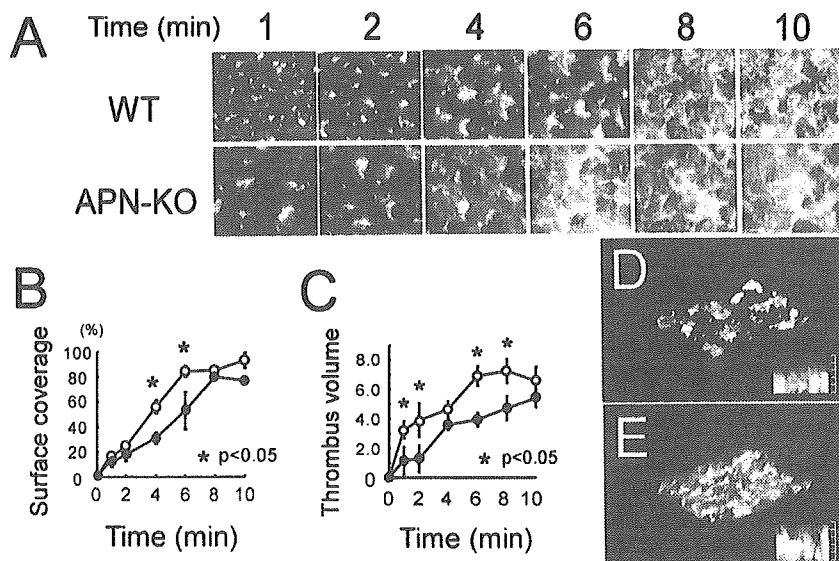

Figure 2. Thrombogenesis on a type I collagen-coated surface under flow conditions. (A) Mepacrine-labeled whole blood obtained from WT (top) or APN-KO mice (bottom) was perfused on a type I collagen-coated surface at a shear rate of 250 s^{-1}. (B) Platelet surface coverage (%) and (C) thrombus volume are shown at indicated time points. (●, WT; ○, APN-KO; *$P<0.05$). Shown are representative 3D images of thrombus formation at 6-minute perfusion in whole blood obtained from (D) WT and (E) APN-KO mice. Each inserted figure shows thrombus height.

10-minute perfusion of mouse whole blood anticoagulated with thrombin inhibitor at a low shear rate (250 s^{-1}). In whole blood obtained from WT mice, the thrombus fully covered the collagen-coated surface after 8 to 10 minutes of perfusion. In contrast, the thrombus grew more rapidly and fully covered the surface at 6 minutes in APN-KO mice. At 1 and 2 minutes of perfusion, there was no apparent difference in the initial platelet adhesion to the collagen surface between WT and APN-KO mice, whereas the platelet aggregate formation was significantly enhanced in APN-KO, even at 1 minute. We additionally examined the possibility that adiponectin might inhibit platelet adhesion onto collagen, because adiponectin binds to collagen types I, III, and V.[23] However, mouse recombinant adiponectin (40 μg/mL) did not inhibit the adhesion of platelets onto collagen, indicating that the inhibitory effect of adiponectin is not mediated by the inhibition of platelet binding to collagen (data not shown). At a high shear rate (1000 s^{-1}), the thrombus grew rapidly and fully covered the surface within 3 to 4 minutes. Under such strong stimuli, we did not detect any difference in thrombus formation between WT and APN-KO mice, probably because of the full activation of platelets.

Adiponectin Inhibits the Enhanced Platelet Aggregation in APN-KO Mice

In platelet aggregation studies, PRP obtained from APN-KO mice showed significantly enhanced platelet aggregation in response to low doses of agonists (ADP 2.5 μmol/L, collagen 2.5 μg/mL, and protease-activated receptor 4–activating peptide [PAR4-TRAP] 75 μmol/L), as compared with WT mice (Figure 3). The maximal platelet aggregation was achieved at higher concentrations of agonists, and the enhanced platelet aggregation in APN-KO mice was not apparent at these high doses of agonists, probably because of the full activation of platelets.

To confirm the inhibitory effect of adiponectin on platelet aggregation in vitro, we mixed 1 volume of PRP obtained from APN-KO mice with 4 volumes of platelet-poor plasma (PPP) obtained from APN-KO mice injected with either Ad-βgal or Ad-APN to adjust platelet counts to $300 \times 10^3/\mu$L. As shown in Figure 4A, the in vitro supplementation of PPP containing adiponectin attenuated the enhanced platelet aggregation. Similarly, in vitro administration of mouse recombinant adiponectin (40 μg/mL) to PRP from APN-KO mice attenuated the enhanced platelet aggregation (Figure 4B).

Expression of Adiponectin Receptors in Platelets and Effects of Adiponectin Deficiency on $\alpha_{IIb}\beta_3$ Activation and P-Selectin Expression

To reveal the effect of adiponectin on platelets, we examined whether platelets possess transcripts for adiponectin receptors AdipoR1 and AdipoR2 by using RT-PCR. As shown in Figure 5A, platelets from APN-KO, as well as WT mice, contained mRNAs for AdipoR1 and AdipoR2. We also confirmed that the human megakaryocytic cell line CMK, as well as carefully isolated human platelets, possessed mRNAs for AdipoR1 and AdipoR[2]. We next examined the effects of adiponectin deficiency on $\alpha_{IIb}\beta_3$ activation and α-granule secretion at various concentrations of agonists by flow
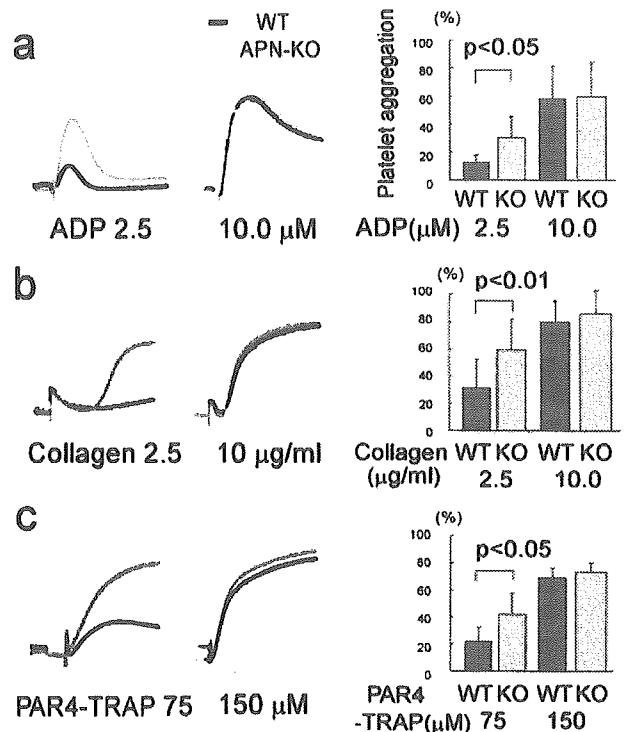

Figure 3. Enhanced platelet aggregation in APN-KO mice. Platelet aggregation in PRP obtained from WT or APN-KO mice. PRP ($300 \times 10^3/\mu$L) obtained from WT (black line) or APN-KO mice (gray line) was stimulated with ADP (a; n=4), collagen (b; n=4), or PAR4-TRAP (c; n=3). As compared with WT mice, platelet aggregation was enhanced in APN-KO mice at low concentrations of agonists.

cytometry. However, neither the platelet $\alpha_{IIb}\beta_3$ activation induced by ADP nor P-selectin expression induced by PAR4-TRAP showed significant difference between WT and APN-KO mice (n=4; Figure 5B and 5C).

Adiponectin Adenovirus Attenuates Thrombus Formation in WT Mice

Because WT mice have large amounts of adiponectin in their plasma, we, therefore, examined whether adiponectin overexpression could additionally inhibit thrombus formation, as well as platelet function, in WT mice. After the administration of Ad-APN or Ad-βgal into WT mice, the plasma adiponectin levels in Ad-APN-infected mice reached $\approx$4 times higher than those in Ad-βgal-infected WT mice (8.5$\pm$0.6 μg/mL for Ad-βgal and 37.0$\pm$14.8 μg/mL for Ad-APN; n=5). As shown in Figure 6A, platelet aggregation in PRP induced by collagen or PAR4-TRAP was significantly attenuated by the overexpression of adiponectin. Similarly, in vitro administration of human recombinant adiponectin (40 μg/mL) to human PRP attenuated the platelet aggregation response to 2.5 μg/mL collagen (Figure 6B). Moreover, in the He-Ne laser–induced carotid artery thrombus model, the overexpression of adiponectin significantly inhibited thrombus formation in WT mice (4.38$\pm$0.75$\times$10^7 arbitrary units for Ad-βgal and 2.75$\pm$0.61$\times$10^7 arbitrary units for Ad-APN; n=7; $P<0.05$; Figure 6C).
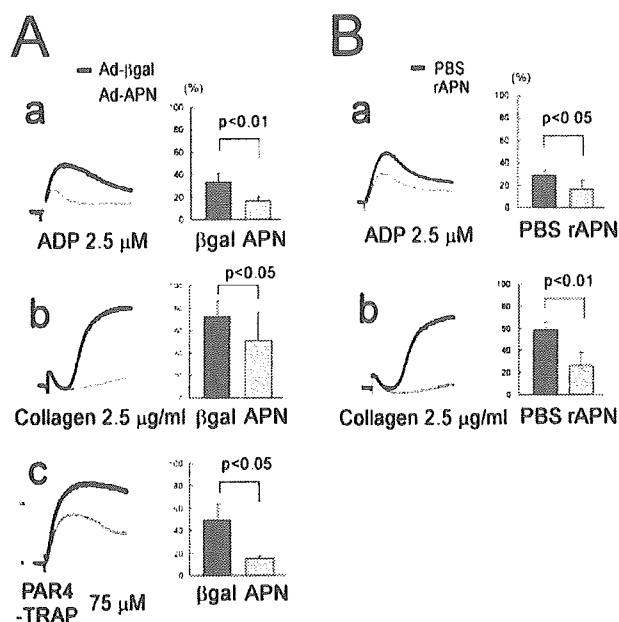
Figure 4. Effects of in vitro supplementation of adiponectin or recombinant adiponectin on the enhanced platelet aggregation in APN-KO mice. (A) One volume of PRP from APN-KO mice was mixed with ≈4 volumes of PPP from APN-KO mice injected with Ad-βgal (black line) or Ad-APN (gray line) to obtain a platelet concentration of $300\times10^3/\mu$L. Platelets were stimulated with indicated agonists (n=4). (B) Mouse recombinant adiponectin (40 μg/mL, gray line) or PBS (black line) was added to PRP from APN-KO mice. Platelets were adjusted to 300×10^3 platelets/μL and stimulated with indicated agonists (n=4).

Discussion

In the present study, we have newly revealed an antithrombotic effect of adiponectin. APN-KO male mice (8 to 12 weeks old) fed on a normal diet showed no significant differences in platelet counts and coagulation parameters compared with WT mice. In the He-Ne laser–induced carotid artery thrombus model, APN-KO mice showed an accelerated thrombus formation, and adenovirus-mediated supplementation of adiponectin attenuated this enhanced thrombus formation. Platelet aggregometry and the real-time observation of in vitro thrombus formation on a type I collagen-coated surface under flow conditions showed the enhanced platelet function in APN-KO mice. Moreover, adenovirus-mediated overexpression of adiponectin attenuated in vivo thrombus formation, as well as the in vitro platelet aggregation response, even in WT mice. Thus, the present data strongly suggest that adiponectin possesses an antithrombotic potency.

We have demonstrated that low concentrations of adiponectin are associated with the prevalence of CAD in men, which is independent of well-known CAD risk factors.[8] Pischon et al[9] have recently shown that high concentrations of adiponectin are associated with a lower risk of myocardial infarction in men, which is also independent of inflammation and glycemic status and can be only partly explained by differences in blood lipids. These clinical studies suggest that the protective effect of adiponectin on the development of CAD may be primary rather than secondary through the protection of metabolic abnormalities, such as insulin resistance. Indeed, APN-KO mice fed on a normal diet did not
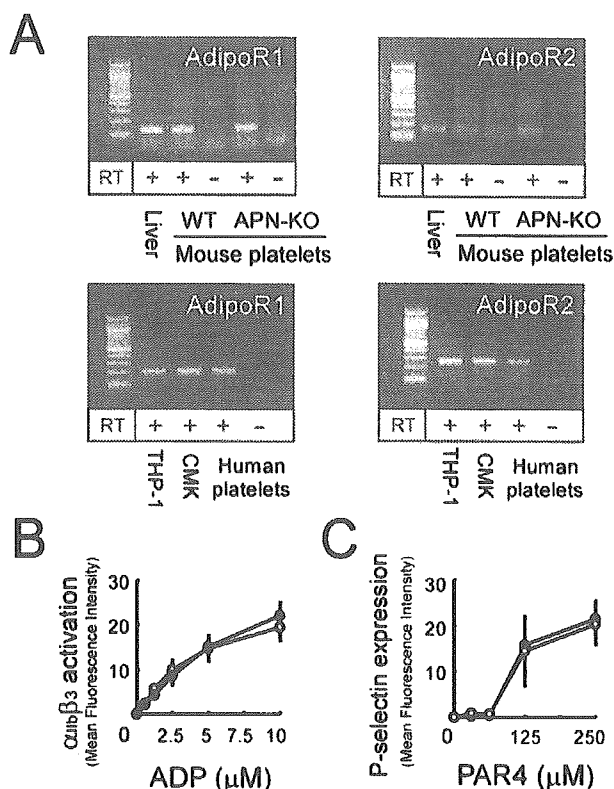

Figure 5. Expression of adiponectin receptors and effects of adiponectin deficiency on platelet function. (A, top) Expressions of transcripts for adiponectin receptors, AdipoR1 (133-bp fragments) and AdipoR2 (156-bp fragments), in platelets from WT or APN-KO mice were examined by RT-PCR. The liver was used as a positive control. (Bottom) Expressions of transcripts for adiponectin receptors, AdipoR1 (196-bp fragments) and AdipoR2 (243-bp fragments), in CMK cells, as well as human platelets, were examined by RT-PCR; 100-bp DNA Ladder (New England Biolabs) was used as a marker. Effects of adiponectin deficiency on (B) $\alpha_{IIb}\beta_3$ activation and (C) α-granule secretion. PRP obtained from WT (●) or APN-KO (○) mice in the presence of phycoerythrin-JON/A mAb or FITC-anti-P-selectin mAb was stimulated with the indicated agonist and then analyzed by flow cytometry without any washing. There were no significant differences in platelet $\alpha_{IIb}\beta_3$ activation or P-selectin expression between WT and APN-KO mice (n=4).

show any abnormalities in plasma glucose, insulin, or lipid profiles.[10,12] Although the atherosclerotic and thrombotic processes are distinct from each other, these processes appear to be interdependent, as shown by the term *atherothrombosis*. The interaction between the vulnerable atherosclerotic plaque, which is prone to disruption, and thrombus formation is the cornerstone of acute coronary syndrome (ACS).[24] In this context, our present data strongly suggest that adiponectin deficiency (or hypoadiponectinemia) may directly contribute to the development of ACS by enhanced platelet thrombus formation.

Although APN-KO fed on a normal diet showed no significant differences in major metabolic parameters, they showed delayed clearance of FFA in plasma, elevated plasma TNF-α concentrations (≈40 pg/mL in APN-KO; ≈20 pg/mL in WT), and elevated CRP mRNA levels in white adipose tissue.[12,25] In addition, recombinant adiponectin increased NO production in vascular endothelial cells.[26] To rule out any
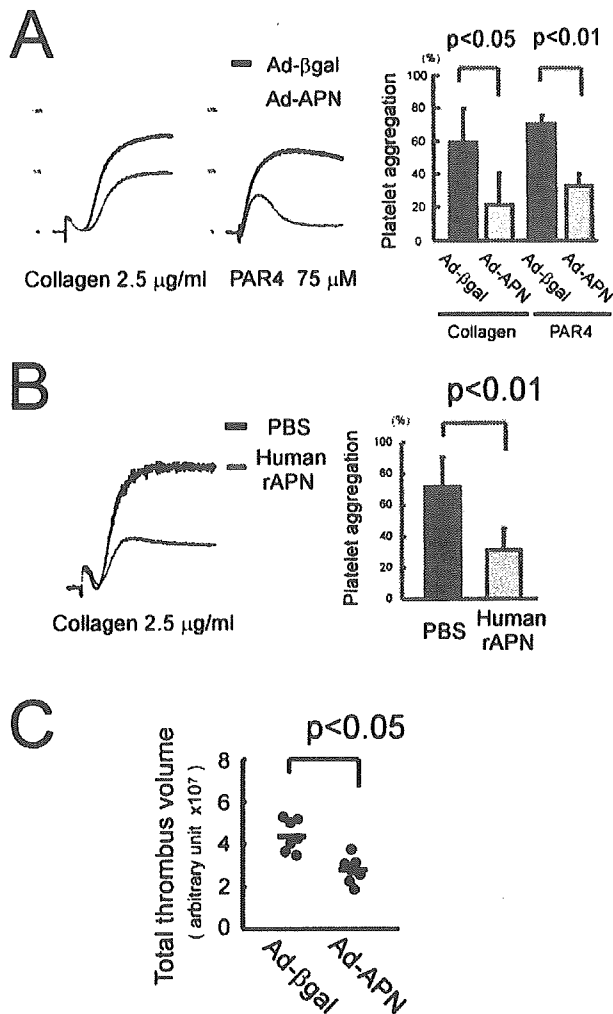
Figure 6. Overexpression of adiponectin additionally attenuates thrombus formation in WT mice. (A) Platelet aggregation in PRP obtained from WT mice injected with either Ad-βgal or Ad-APN. PRP (300×10³/μL) obtained from WT mice injected with either Ad-βgal (black line) or Ad-APN (gray line) was stimulated with collagen or PAR4-TRAP (n=4). Administration of Ad-APN significantly attenuated platelet aggregation in WT mice. (B) Human recombinant adiponectin (40 μg/mL, gray line) or PBS (black line) was added to PRP (300×10³/μL) from control subjects. Platelets were stimulated with collagen (n=7). (C) He-Ne laser–induced thrombus formation in WT mice injected with either Ad-βgal or Ad-APN. Administration of Ad-APN in WT mice additionally reduced the total thrombus volume in the carotid artery thrombus model (n=7, P<0.05).

effect of adiponectin on vascular cells, we examined in vitro thrombus formation on a type I collagen-coated surface under flow conditions, as well as platelet aggregation in APN-KO mice. Thus, the enhanced platelet function in APN-KO mice was still evident even in the absence of vascular cells. Moreover, human and mouse recombinant adiponectin attenuated the aggregation response obtained from control human subjects and from APN-KO mice, respectively. Thus, adiponectin inhibits platelet function. However, the mechanism by which adiponectin attenuates platelet aggregation and arterial thrombus formation in vivo remains unclear. During thrombogenesis, platelets adhere to altered vascular surfaces or exposed subendothelial matrices, such as collagen, and

then become activated and aggregate to each other.[16] The thrombus formed in APN-KO mice appeared to be stable and more resistant to the increased shear stress, without affecting the initiation time for thrombus formation in carotid artery injury experiments, as well as in flow chamber perfusion experiments. In addition, preincubation of collagen with recombinant adiponectin did not inhibit platelet adhesion on collagen under static conditions. Thus, it is unlikely that the inhibitory effect of adiponectin is mediated by the inhibition of platelet binding to collagen. These characteristics are quite distinct from C1q-TNF–related protein-1, which belongs to the same family as adiponectin and inhibits thrombus formation by interfering with platelet–collagen interaction.[27] We confirmed that transcripts for AdipoR1 and AdipoR2 were present in mouse and human platelets and CMK cells. Although the platelet–platelet interaction appeared to be enhanced in APN-KO mice, we did not detect any difference in agonist-induced $\alpha_{IIb}\beta_3$ activation or P-selectin expression between APN-KO and WT mice by flow cytometry. Based on these results, it is possible that adiponectin may inhibit $\alpha_{IIb}\beta_3$-mediated intracellular postligand binding events. Alternatively, previous studies have shown that adiponectin is physically associated with many proteins, including α_2-macroglobulin, thrombospondin-1 (TSP-1), and several growth factors.[5,23,28] Interestingly, TSP-1, after secretion from platelet α granules, may participate in platelet aggregation by reinforcing interplatelet interactions through direct fibrinogen-TSP-fibrinogen and TSP-TSP crossbridges.[29,30] In this context, it is also possible that it may interfere with interplatelet interactions in platelet aggregation. Additional studies to clarify the mechanism of adiponectin are currently under way.

In conclusion, our present study revealed that adiponectin acts as an endogenous antithrombotic factor. Although it is possible that the in vivo antithrombotic effect of adiponectin may be partly mediated by its action on vascular cells, our present data clearly indicate that adiponectin affects platelet function in the absence of vascular cells. In addition, the overexpression of adiponectin in WT mice attenuates in vivo thrombus formation, as well as the in vitro platelet aggregation response. Our data provide a new insight into the pathophysiology of ACS in nonobese, as well as obese, subjects, and adiponectin (and its derivatives) may be a new candidate for an antithrombotic drug.

References

1. Spiegelman BM, Flier JS. Obesity and the regulation of energy balance. Cell. 2001;104:531–543.

2. Friedman JM. Obesity in the new millennium. Nature. 2000;404: 632–634.

3. Hotamisligil GS, Shargill NS, Spiegelman BM. Adipose expression of tumor necrosis factor-α: direct role in obesity-linked insulin resistance. Science. 1993;259:87–91.

4. Steppan CM, Bailey ST, Bhat S, Brown EJ, Banerjee RR, Wright CM, Patel HR, Ahima RS, Lazar MA. The hormone resistin links obesity to diabetes. *Nature*. 2001;409:307–312.

5. Matsuzawa Y, Funahashi T, Kihara S, Shimomura I. Adiponectin and metabolic syndrome. *Arterioscler Thromb Vasc Biol*. 2004;24:29–33.

6. Hotta K, Funahashi T, Arita Y, Takahashi M, Matsuda M, Okamoto Y, Iwahashi H, Kuriyama H, Ouchi N, Maeda K, Nishida M, Kihara S, Sakai N, Nakajima T, Hasegawa K, Muraguchi M, Ohmoto Y, Nakamura T, Yamashita S, Hanafusa T, Matsuzawa Y. Plasma concentrations of a novel, adipose-specific protein, adiponectin, in type 2 diabetic patients. *Arterioscler Thromb Vasc Biol*. 2000;20:1595–1599.

7. Zoccali C, Mallamaci F, Tripepi G. Novel cardiovascular risk factors in end-stage renal disease. *J Am Soc Nephrol*. 2002;13:134–141.

8. Kumada M, Kihara S, Sumitsuji S, Kawamoto T, Matsumoto S, Ouchi N, Arita Y, Okamoto Y, Shimomura I, Hiraoka H, Nakamura T, Funahashi T, Matsuzawa Y. Association of hypoadiponectinemia with coronary artery disease in men. *Arterioscler Thromb Vasc Biol*. 2003;23:85–89.

9. Pischon T, Girman CJ, Hotamisligil GS, Rifai N, Hu FB, Rhimm EB. Plasma adiponectin levels and risk of myocardial infarction in men. *JAMA*. 2004;291:1730–1737.

10. Maeda N, Shimomura I, Kishida K, Nishizawa H, Matsuda M, Nagaretani H, Furuyama N, Kondo H, Takahashi M, Arita Y, Komuro R, Ouchi N, Kihara S, Tochino Y, Okutomi K, Horie M, Takeda S, Aoyama T, Funahashi T, Matsuzawa Y. Diet-induced insulin resistance in mice lacking adiponectin/ACRP30. *Nat Med*. 2002;8:731–737.

11. Yokota T, Oritani K, Takahashi I, Ishikawa J, Matsuyama A, Ouchi N, Kihara S, Funahashi T, Tenner AJ, Tomiyama Y, Matsuzawa Y. Adiponectin, a new member of the family of soluble defense collagens, negatively regulates the growth of myelomonocytic progenitors and the functions of macrophages. *Blood*. 2000;96:1723–1732.

12. Matsuda M, Shimomura I, Sata M, Arita Y, Nishida M, Maeda N, Kumada M, Okamoto Y, Nagaretani H, Nishizawa H, Kishida K, Komuro R, Ouchi N, Kihara S, Nagai R, Funahashi T. Role of adiponectin in preventing vascular stenosis. *J Biol Chem*. 2002;277:37487–37491.

13. Okamoto Y, Kihara S, Ouchi N, Nishida M, Arita Y, Kumada M, Ohashi K, Sakai N, Shimomura I, Kobayashi H, Terasaka N, Inaba T, Funahashi T, Matsuzawa Y. Adiponectin reduces atherosclerosis in apolipoprotein E-deficient mice. *Circulation*. 2002;106:2767–2770.

14. Kato H, Honda S, Yoshida H, Kashiwagi H, Shiraga M, Honma N, Kurata Y, Tomiyama Y. SHPS-1 negatively regulates integrin $\alpha_{IIb}\beta_3$ function through CD47 without disturbing FAK phosphorylation. *J Thromb Haemost*. 2005;3:763–774.

15. Sano T, Oda E, Yamashita T, Shiramasa H, Ijiri Y, Yamashita T, Yamamoto J. Antithrombotic and anti-atherogenic effects of partially defatted flaxseed meal using a laser-induced thrombosis test in apolipoprotein E and low-density lipoprotein receptor deficient mice. *Blood Coagul Fibrinolysis*. 2003;14:707–712.

16. Tsuji S, Sugimoto M, Miyata S, Kuwahara M, Kinoshita S, Yoshioka A. Real-time analysis of mural thrombus formation in various platelet aggregation disorders: distinct shear-dependent roles of platelet receptors and adhesive proteins under flow. *Blood*. 1999;94:968–975.

17. Ouchi N, Kobayashi H, Kihara S, Kumada M, Sato K, Inoue T, Funahashi T, Walsh K. Adiponectin stimulates angiogenesis by promoting cross-talk between AMP-activated protein kinase and Akt signaling in endothelial cells. *J Biol Chem*. 2004;279:1304–1309.

18. Tomiyama Y, Kashiwagi H, Kosugi S, Shiraga M, Kanayama Y, Kurata Y, Matsuzawa Y. Abnormal processing of the glycoprotein IIb transcript due to a nonsense mutation in exon 17 associated with Glanzmann's thrombasthenia. *Thromb Haemost*. 1995;73:756–762.

19. Yamauchi T, Kamon J, Ito Y, Tsuchida A, Yokomiza T, Kita S, Sugiyama T, Miyagishi M, Hara K, Tsunoda M, Murakami K, Ohteki T, Uchida S, Takekawa S, Waki H, Tsuno NH, Shibata Y, Terauchi Y, Froguel P, Tobe K, Koyasu S, Taira K, Kitamura T, Shimizu T, Nagai R, Kadowaki T. Cloning of adiponectin receptors that mediate antidiabetic metabolic effects. *Nature*. 2003;423:762–769.

20. Bluher M, Fasshauer M, Kralisch S, Schon MR, Krohn K, Paschke R. Regulation of adiponectin receptor R1 and R2 gene expression in adipocytes of C57BL/6 mice. *Biochem Biophys Res Commun*. 2005;329:1127–1132.

21. Kashiwagi H, Honda S, Tomiyama Y, Mizutani H, Take H, Honda Y, Kosugi S, Kanayama Y, Kurata Y, Matsuzawa Y. A novel polymorphism in glycoprotein IV (replacement of proline-90 by serine) predominates in subjects with platelet GPIV deficiency. *Thromb Haemost*. 1993;69:481–484.

22. Chinetti G, Zawadski C, Fruchart JC, Staels B. Expression of adiponectin receptors in human macrophages and regulation by agonists of the nuclear receptors PPARα, PPARγ, and LXR. *Biochem Biophys Res Commun*. 2004;314:151–158.

23. Okamoto Y, Arita Y, Nishida M, Muraguchi M, Ouchi N, Takahashi M, Igura T, Inui Y, Kihara S, Nakamura T, Yamashita S, Miyagawa J, Funahashi T, Matsuzawa Y. An adipocyte-derived plasma protein, adiponectin, adheres to injured vascular walls. *Horm Metab Res*. 2000;32:47–50.

24. Fuster V, Badimon L, Badimon JJ, Chesebro JH. The pathogenesis of coronary artery disease and the acute coronary syndromes. *N Engl J Med*. 1992;326:242–250.

25. Ouchi N, Kihara S, Funahashi T, Nakamura T, Nishida M, Kumada M, Okamoto Y, Ohashi K, Nagaretani H, Kishida K, Nishizawa H, Maeda N, Kobayashi H, Hiraoka H, Matsuzawa Y. Reciprocal association of C-reactive protein with adiponectin in blood stream and adipose tissue. *Circulation*. 2003;107:671–674.

26. Chen H, Montagnant M, Funahashi T, Shimomura I, Quon MJ. Adiponectin stimulates production of nitric oxide in vascular endothelial cells. *J Biol Chem*. 2003;278:45021–45026.

27. Meehan WP, Knitter GH, Lasser GW, Lewis K, Ulla MM, Bishop PD, Hanson SR, Fruebis J. C1q-TNF related protein-1 (CTRP1) prevents thrombus formation in non-human primates and atherosclerotic rabbits without causing bleeding. *Blood* 2002;100:23a.

28. Wang Y, Lam KS, Xu JY, Lu G, Xu LY, Cooper GJ, Xu A. Adiponectin inhibits cell proliferation by interacting with several growth factors in an oligomerization-dependent manner. *J Biol Chem*. 2005;280:18341–18347.

29. Leung LL. Role of thrombospondin in platelet aggregation. *J Clin Invest*. 1984;74:1764–1772.

30. Bonnefoy A, Hantgan R, Legrand C, Frojmovic MM. A model of platelet aggregation involving multiple interactions of thrombospondin-1, fibrinogen, and GPIIbIIIa receptor. *J Biol Chem*. 2001;276:5605–5612.

Original Article

NDT

Nephrology Dialysis Transplantation

Novel compound heterozygote mutations (H234Q/R1206X) of the *ADAMTS13* gene in an adult patient with Upshaw–Schulman syndrome showing predominant episodes of repeated acute renal failure

Yugo Shibagaki[1], Masanori Matsumoto[2], Koichi Kokame[3], Shigeyoshi Ohba[1], Toshiyuki Miyata[3], Yoshihiro Fujimura[2] and Toshiro Fujita[1]

[1]Department of Nephrology and Endocrinology, Graduate School of Medicine, University of Tokyo, Tokyo, [2]Department of Blood Transfusion Medicine, Nara Medical University, Nara and [3]National Cardiovascular Center Research Institute, Osaka, Japan

Abstract

Background. Unlike acquired thrombotic thrombocytopenic purpura or haemolytic uraemic syndrome, which are often intractable, thrombotic microangiopathy in patients with Upshaw–Schulman syndrome (USS) – a congenital deficiency of von Willebrand factor-cleaving protease (ADAMTS13) activity – responds very well to plasma infusion and does not even require plasma exchange. However, the symptoms significantly vary in each individual and thus clinicians often overlook this diagnosis.

Methods. A 31-year-old adult male patient with thrombotic microangiopathy, which was complicated with repeated episodes of acute renal failure, is reported. We suspected that the patient had USS and performed assays of ADAMT13 activity and its inhibitor, followed by *ADAMTS13* gene analysis of the patient and his parents.

Results. The patient had extremely low ADAMTS13 activity and has no inhibitors of ADAMTS13. Through an *ADAMTS13* gene analysis of this family, we found two novel mutations responsible for the disease: a missense mutation in exon 7 [702 C→A (H234Q)] from the father and a nonsense mutation in exon 26 [3616 C→T (R1206X)] from the mother.

Conclusions. Our experience appears to indicate the importance of assays of ADAMTS13 activity and its inhibitor in patients who have episodes of renal insufficiency in association with thrombotic microangiopathy, for diagnosis and choice of treatment.

Keywords: acute renal failure; genetic disorder; haemolytic uraemic syndrome; thrombotic microangiopathy; von Willebrand factor

Introduction

Thrombotic thrombocytopenic purpura (TTP) and haemolytic uraemic syndrome (HUS) are both categorized within thrombotic microangiopathy (TMA), featured by microangiopathic haemolytic anaemia with thrombocytopenia [1]. The term TTP typically refers to a form of TMA that affects adolescents and adults and predominantly causes central nervous system disorders, whereas HUS refers to TMA, which mainly involves kidney and typically affects young children with diarrhoea caused by *Escherichia coli* O157:H7 infection. TTP and HUS are mostly indistinguishable by laboratory findings and pathology and thus in clinical practice are often referred to as HUS/TTP [2]. It has, however, been recognized that some forms of TTP respond well to plasma infusion (PI) [3] or plasma exchange (PE), whereas typical diarrhoea-associated HUS does not [4]. Recently, the plasma activity of von Willebrand factor (VWF)-cleaving protease (ADAMTS13, a disintegrin and metalloprotease domain, with thrombospondin type 1 motif 13) was found to be deficient in an inherited form of TTP, which differs from acquired idiopathic TTP characterized by its neutralizing or non-neutralizing inhibitor and from acquired HUS by subnormal enzyme activity [4–6]. If the onset of this inherited form of TTP is in the neonatal period, it is alternatively called Upshaw–Schulman

Correspondence and offprint requests to: Yugo Shibagaki, 7-3-1 Hongo Bunkyo-ku, Tokyo 113-8655, Japan.
Email: eugo@wc4.so-net.ne.jp

syndrome (USS), although there is also an adult onset form of the disease [7].

Subjects and methods

Patient

A 31-year-old male was admitted to the nephrology service for acute renal failure, microangiopathic haemolytic anaemia and thrombocytopenia.

He had a history of moderate jaundice as a newborn, which was treated with phototherapy. At 3 months of age, he had episodes of purpura and thrombocytopenia after diphtheria/pertussis/tetanus immunization, for which he was diagnosed with idiopathic thrombocytopenic purpura. Since the age of 2 years, he had an episode of intracranial bleeding after minor head injury and several episodes of high-renin hypertension and acute renal failure complicated with TMA, all of which were successfully treated with PI. Since then he has been treated with PI every other week to maintain blood platelet count >2 10^9/l, by which he was diagnosed by a previous paediatrician with recurrent HUS/TTP of unknown aetiology.

On admission, he showed no neurological deficits or any other specific symptoms, but subsequently his serum creatinine progressively rose from 0.87 to 5.78 mg/dl with increased LDH (1968 IU/l), low platelet count (3.5 10^9/l) and the presence of schistocytes. However, with PI, LDH rapidly fell back to normal level and his renal dysfunction and thrombocytopenia gradually resolved. He had no apparent family history of congenital coagulopathy, but his elder brother, who died at the age of 2 years, had laboratory data compatible with TMA, which raised our suspicion of the presence of hereditary HUS/TTP, such as USS.

We subsequently performed assays of ADAMTS13 activity, followed by *ADAMTS13* gene analysis of the patient and his parents.

Assay of ADAMTS13 activity and its inhibitor

Plasma ADAMTS13 activity was assayed by the method of Furlan *et al.* [5] based on VWF multimer analysis, with a slight modification as described before [8]. The ADAMTS13 activity of pooled normal plasma was defined as 100%. The normal range of ADAMTS13 activity was 102 ± 23% (mean ± SD) [9].

The inhibitor activity against ADAMTS13 was measured as described by Furlan *et al.* [10] based on the Bethesda method [3]. One unit of inhibitor was defined as the amount that reduced the ADAMTS13 activity to 50% of the control.

ADAMTS13 gene analysis

After obtaining approval from the ethics committees of both the sample-collecting hospital and gene analysis institute, and informed consent, *ADAMTS13* genes of the patient and his parents were analysed by DNA sequencing. All 29 exons and exon–intron boundary sites of the *ADAMTS13* gene were amplified and sequenced as recently described [11].

Results

ADAMTS13 activity of the patient's plasma, which was obtained on admission (and just before PI), was <3% of the pooled normal plasma (Figures 1 and 2) and its inhibitor was undetectable (<0.5 Bethesda U/ml). Three novel mutations were identified (Figure 1). The patient had compound heterozygous mutations comprised of a missense mutation in exon 7 [702 C → A (H234Q)] inherited from his father and a nonsense mutation in exon 26 [3616 C → T (R1206X)] inherited from his mother. His father had an additional missense mutation at exon 21 [2708 C → T (S903L)], but its effect on ADAMTS13 activity is presently unknown [11,12]. Thus, on this occasion, a solid diagnosis of USS was made. Although the patient's parents had heterozygous mutations and relatively low ADAMTS13 activity (father: 24%, mother: 21%; Figure 2), they had no episode of haematological problems and, to date, have been in good health. To investigate the frequencies of these mutations, we sequenced the relevant exons of ADAMTS13 in
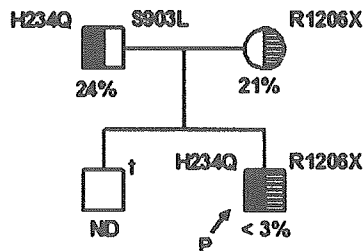

Fig. 1. Pedigree of the index patient with gene haplotypes and plasma activity of ADAMTS13. The circle represents a female and squares represent males. Plasma ADAMTS13 activity (%) is shown under the circle and the squares. Mutations found in the *ADAMTS13* gene are shown as one-letter amino acid abbreviations numbered from the initial Met codon. The arrow indicates the index patient. Both the mother and the father of the index patient are asymptomatic carriers. †A deceased individual. P, index patient; ND; value not determined.
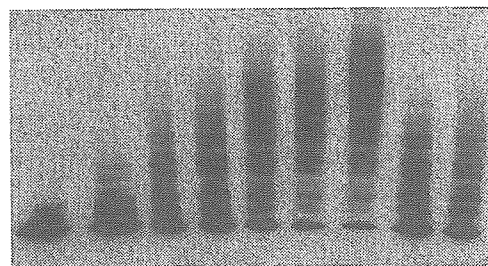
Fig. 2. Cleavage of VWF multimer by ADAMTS13. Quantitative assay of plasma ADAMTS13 activity from a control, the patient and the parents. Following incubation of VWF, plasma from six dilution series of a normal control and plasma from the patient and his parents, sodium dodecyl sulphate–agarose gel electrophoresis and western blotting were performed as shown in a previous report [8]. The plasma ADAMTS13 activity was shown as a percentage of the normal control.